Czech Technical University in Prague
Faculty of Nuclear Sciences and Physical Engineering

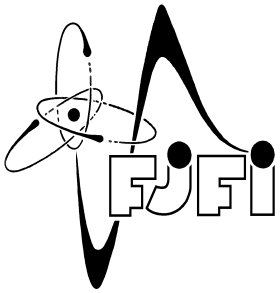

DIPLOMA THESIS

Bc. Lucie Augustovičová

Supervisor: Doc. Ing. Pavel Soldán, Dr.

May 5, 2011

Acknowledgments

I would like to thank doc. Pavel Soldán for many illuminating discussions, his outstanding support and for his careful reading of this manuscript. Especially, I appreciate his perfect supervision during the past three years. I am also grateful to Dr. Vladimír Špirko for his kind financial support.

Název práce: **Radiativní asociace atomů**

Autor: Lucie Augustovičová

Obor: Matematické inženýrství

Zaměření: Matematická fyzika

Druh práce: Diplomová práce

Vedoucí práce: doc. Ing. Pavel Soldán, Dr., Univerzita Karlova v Praze, Matematicko-fyzikální fakulta, Katedra chemické fyziky a optiky, Ke Karlovu 3, 121 16 Praha 2

Abstrakt: Tato práce se zabývá jevem radiativní asociace v případě dvouatomových molekul. Úloha potenciálové bariéry v rezonančním rozptylu je krátce diskutována na modelovém příkladě. Hönlovy-Londonovy koeficienty pro přechody s dipólovým a kvadrupólovým momentem jsou odvozeny. Proces radiativní asociace $\mathrm{Li}^+(1s^2)+\mathrm{He}(1s^2)$ vedoucí ke vzniku molekulárního iontu $\mathrm{LiHe}^+(X\,^1\Sigma^+)$ je vyšetřován. Výpočet účinných průřezů pro přímou radiativní asociaci $\mathrm{LiHe}^+(X\,^1\Sigma^+)$ je podrobně popsán.

Klíčová slova: radiativní asociace, Hönlovy-Londonovy faktory, Einsteinovy koeficienty, účinný průřez

Title: **Radiative association of atoms**

Author: Lucie Augustovičová

Abstract: This thesis deals with the phenomenon of radiative association in the case of diatomic molecules. The role of potential barrier in a resonance scattering is briefly discussed on a model example. Hönl-London coefficients for dipole moment and quadrupole moment transitions are derived. The process of radiative association of $\mathrm{Li}^+(1s^2)+\mathrm{He}(1s^2)$ leading to the formation of the molecular ion $\mathrm{LiHe}^+(X\,^1\Sigma^+)$ is investigated. Evaluation of the cross sections for direct radiative association of $\mathrm{LiHe}^+(X\,^1\Sigma^+)$ is described in detail.

Key words: radiative association, Hönl-London factors, Einstein coefficients, cross section

Contents

List of Figures

List of Tables

Introduction

Radiative association is an important process in the gas phase chemistry of interstellar clouds [19, 8]. The first galaxies and stars were formed from a gas of H and ^{4}He with trace amounts of D, ^{3}He and ^{7}Li [23]. The scale of the first cosmological objects formed in the Universe was controlled by cooling, and it is often molecular cooling that allows primordial clouds to collapse. Therefore the study of the first molecules formation by radiative processes in primordial gases is important [13, 25, 3, 9, 22]. Radiative association of $Li^+ + He$, which is considered in this thesis, has not been studied yet.

Let us present the brief overview of the contents of this diploma thesis. In Chapter 1 we show that a potential barrier leads to shape resonances in the problem of resonance scattering by a model repulsive barrier. Quasi-stationary levels are located using a boundary condition method, the corresponding wave functions and other characteristics will be found.

In Chapter 2 we derive the multipole line strength for Hund's case (a) linear molecules through the use of Clebsch-Gordan angular momentum coupling coefficients. We treat all the basic concepts of electric transitions using a quadrupole moment terminology, which is rarely discussed in the literature.

The Chapter 3 deals with direct radiative association, which can occur when a pair of atomic species approaches along potential energy curve with a relative energy forming initially a collision complex. This unstable complex, generally considered to exist in the vibrational continuum of the ground/excited electronic state, decays to a vibrational-rotational level of a lower bound electronic state. Radiative association can proceed by spontaneous emission of a photon with energy equal to $h\nu$. We summarize the relevant theory and carry out explicit calculations of the cross sections for the radiative association of $Li^+(1s^2) + He(1s^2)$. These results are obtained using a fully quantum mechanical method. Computations are carried out in the programming language FORTRAN 95.

Chapter 1

Resonant scattering by a repulsive barrier

In this chapter we shall discuss resonances in atoms/molecules, that is, states which can be regarded as a temporary bound state capable of decaying by particle emission. For a resonance to occur there are different mechanisms for retaining a projectile in the target. A simple mean by which the projectile is trapped is a potential barrier. Let us suppose that the incident particle experiences a region of attractive potential surrounded by a region of repulsive potential. If the particle enters the region of attractive potential, the surrounding potential barrier will hinder its escape. The most common cause of a barrier is the centrifugal potential, but there are also many potential curves which have barrier even for zero angular momentum. Resonances which are supported by potential barriers are called shape resonances.

The best-known example is the radioactive nuclei which decay by the emission of an α-particle which has tunnelled through the Coulomb barrier. The potential energy of an α-particle in the field of a nucleus consists of two parts, the attractive potential due to the short-range nuclear forces, and the potential barrier produced by the Coulomb repulsion between protons and by the centrifugal force. The emission of an α-particle is represented as a specific quantum phenomenon resulting from the transparency of the barrier.

The potential necessary for the existence of shape resonances can be found in both nuclear and molecular systems. In atomic and molecular systems the attractive potential is due to the Coulomb attraction of electrons and protons, whereas the barrier is normally caused by the centrifugal force.

1.1 Theoretical model

Let us consider a model with a spherically symmetric repulsive shell potential of a simplified shape

$$U(r) = \begin{cases} 0 & 0 < r < r_1\,, \\ U_0 & r_1 \le r \le r_2\,, \\ 0 & r_2 < r. \end{cases}$$

The incident motion is assumed to be in the z direction, angular momentum is conserved, the radial part of the wave function satisfies one-dimensional equation

$$-\frac{\hbar^2}{2m}\left[\frac{\mathrm{d}^2}{\mathrm{d}r^2} + \frac{2}{r}\frac{\mathrm{d}}{\mathrm{d}r} + V_L(r)\right] R(r) = ER(r), \qquad r \ge 0, \tag{1.1}$$

where

$$V_L(r) = \frac{\hbar^2}{2m}\frac{L(L+1)}{r^2} + U(r)\,.$$

and m is the mass of a particle. By substituting $R(r) = \psi(r)/r$ equation (1.1) is simplified to the one-dimensional radial Schrödinger equation of the form

$$\left[-\frac{\hbar^2}{2m}\frac{\mathrm{d}^2}{\mathrm{d}r^2} + V_L(r)\right]\psi(r) = E\psi(r)\,. \tag{1.2}$$

One boundary condition being $\psi(0) = 0$, the other condition is not imposed forasmuch as in the range of large values of the independent variable the solution of the Schrödinger equation exhibits sinusoidal behaviour.

In the region I the wave function vanishing for $r = 0$ has the form

$$\psi(r) = A\sin kr\,, \qquad k^2 = \frac{2ME}{\hbar^2}\,.$$

In the region II the general solution with respect to $r - r_1$ is

$$\psi(r) = B_+ e^{\kappa(r-r_1)} + B_- e^{-\kappa(r-r_1)}\,, \qquad \kappa^2 = \frac{2M(U_0 - E)}{\hbar^2}\,.$$

For the wave function in the region III, where once again $U = 0$, we have

$$\psi(r) = C_+ e^{ik(r-r_2)} + C_- e^{-ik(r-r_2)}\,.$$

The coefficients B_+, B_-, C_+, C_- are determined from the continuity condition of the wave function and its first derivative. At the boundary of regions I and II these conditions lead to the relations

$$\begin{aligned} A\sin kr_1 &= B_+ + B_-\,, \\ Ak\cos kr_1 &= \kappa(B_+ - B_-)\,, \end{aligned}$$

whence

$$B_+ = \frac{1}{2}A\left(\sin kr_1 + \frac{k}{\kappa}\cos kr_1\right),$$
$$B_- = \frac{1}{2}A\left(\sin kr_1 - \frac{k}{\kappa}\cos kr_1\right). \tag{1.3}$$

Similarly, at the boundary of regions II and III we have

$$B_+ e^{\kappa(r_2-r_1)} + B_- e^{-\kappa(r_2-r_1)} = C_+ + C_-,$$
$$\kappa\left(B_+ e^{\kappa(r_2-r_1)} - B_- e^{-\kappa(r_2-r_1)}\right) = \mathrm{i}k(C_+ - C_-).$$

From the latter equations, we find C_+ and C_- in terms of A:

$$C_+ = \frac{1}{4}A\sin kr_1\left(1+\frac{\kappa}{\mathrm{i}k}\right)e^{\kappa(r_2-r_1)}\left[1+\frac{1-\frac{\kappa}{\mathrm{i}k}}{1+\frac{\kappa}{\mathrm{i}k}}e^{-2\kappa(r_2-r_1)}+\right.$$
$$\left.+\frac{k}{\kappa}\cot kr_1\left(1-\frac{1-\frac{\kappa}{\mathrm{i}k}}{1+\frac{\kappa}{\mathrm{i}k}}e^{-2\kappa(r_2-r_1)}\right)\right],$$
$$C_- = \frac{1}{4}A\sin kr_1\left(1-\frac{\kappa}{\mathrm{i}k}\right)e^{\kappa(r_2-r_1)}\left[1+\frac{1+\frac{\kappa}{\mathrm{i}k}}{1-\frac{\kappa}{\mathrm{i}k}}e^{-2\kappa(r_2-r_1)}+\right. \tag{1.4}$$
$$\left.+\frac{k}{\kappa}\cot kr_1\left(1-\frac{1+\frac{\kappa}{\mathrm{i}k}}{1-\frac{\kappa}{\mathrm{i}k}}e^{-2\kappa(r_2-r_1)}\right)\right].$$

The formulae (1.3) and (1.4) constitute the stationary wave function corresponding to the energy E which largely influences the behavior of the wave function for the particle. We shall consider the limiting case $\kappa(r_2 - r_1) \gg 1$. Then we may neglect all the terms containing the factor $e^{-2\kappa(r_2-r_1)}$ and the coefficients will then have the form

$$C_+ \approx \frac{1}{4}A\sin kr_1\left(1+\frac{\kappa}{\mathrm{i}k}\right)e^{\kappa(r_2-r_1)}\left(1+\frac{k}{\kappa}\cot kr_1\right), \quad C_- = C_+^*.$$

The quantity of C_+ and C_- compared to A depends to a great extent on the expression $1 + (k/\kappa)\cot kr_1$. For certain values of the energy called the quasi-stationary levels, which lie in the vicinity of the roots of the transcendental equation

$$1 + \sqrt{\frac{E_n}{U_0 - E_n}}\cot\frac{\sqrt{2ME_n}}{\hbar}r_1 = 0, \tag{1.5}$$

the coefficients C_+, C_- are considerably smaller than A.

It may readily be shown from the condition of continuity ψ and ψ' and from the boundary condition for large r that the roots of Eq. (1.5) are bound states for a particle in the potential shown in Fig. 1.1 ($r_2 \to \infty$).

1.2 Numerical results

In our numerical study we consider a particular rectangular barrier with the parameters $U_0 = 1\,\mathrm{eV}$, $r_1 = 10^{-9}\,\mathrm{m}$, $r_2 = 2\times10^{-9}\,\mathrm{m}$. Numerical computation with electron mass $0.510998910\,\mathrm{MeV/c^2}$ gives quasi-energy levels of $E_{\mathrm{res1}} = 0.259051096847\,\mathrm{eV}$ and $E_{\mathrm{res2}} = 0.947017018143\,\mathrm{eV}$ (Fig. 1.2) which are found when the expression in the square brackets of (1.4) vanishes. These values were obtained using the software Maple 11, specifically the "fsolve" command. Solving Eq. (1.5) gives $E_1 = 0.259061203092\,\mathrm{eV}$ and $E_2 = 0.938471516153\,\mathrm{eV}$.

Therefore the wave functions corresponding to the values of the energies in the narrow band in the vicinity of the quasi-levels are suppressed by the potential barrier in the region III (see Fig. 1.3a). This effect of resonant behavior becomes particularly evident in Fig. 1.4b and 1.5a, in which the wave functions are shown at fixed resonance energies E_{res1} and E_{res2}.

Figures 1.3b, 1.5b and 1.3c, 1.5c illustrate the behavior of wave functions for the external quasi-bound region. The dominant amplitude shifts to the region III, where the wave function differs significantly from zero as seen in Fig. 1.3c and 1.5c. Finally, note the sharp variation in the amplitudes and the change of π in the phase shift when passing through the resonance point $E = E_{\mathrm{res1}}$ in Fig. 1.4.

The results shown in Figures (1.3a) and (1.4b) indicate that the first (lower) resonance is well localized by the formula (1.5) which is in agreement with the assumption $\kappa(r_2 - r_1) \gg 1$. For the second (higher) resonance, this assumption can not be used to simplify Eq. (1.4).

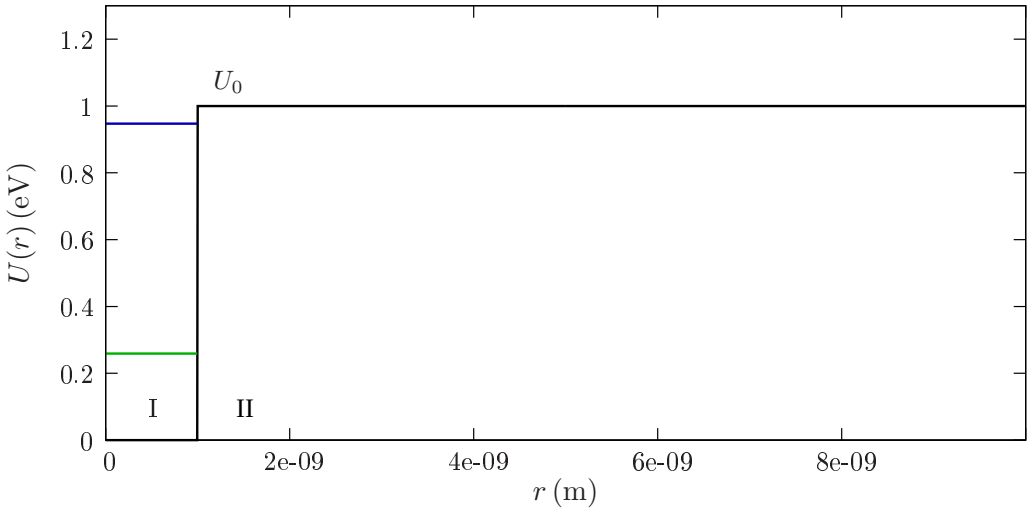

Figure 1.1: Schematic diagram of a potential barrier with its bound states.

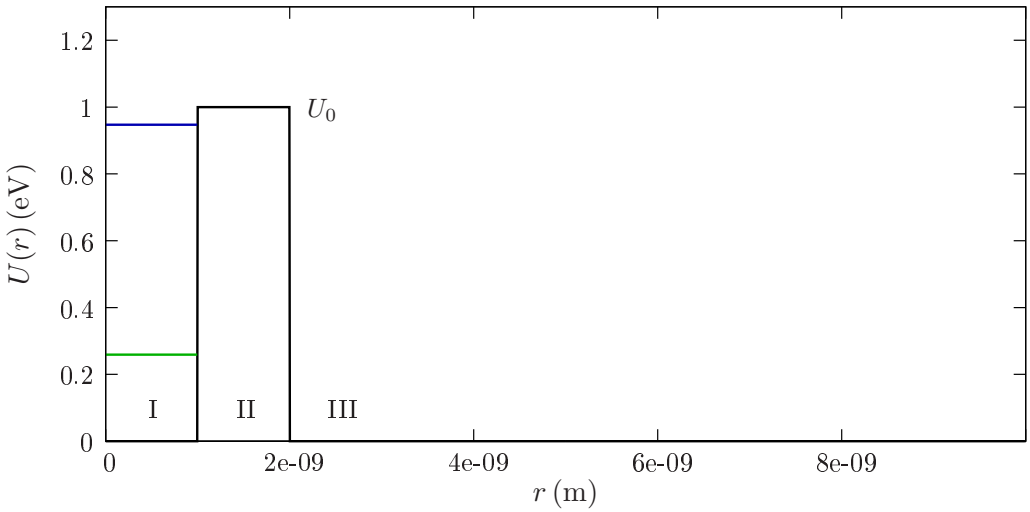

Figure 1.2: Plot of the potential barrier with its quasi-levels.

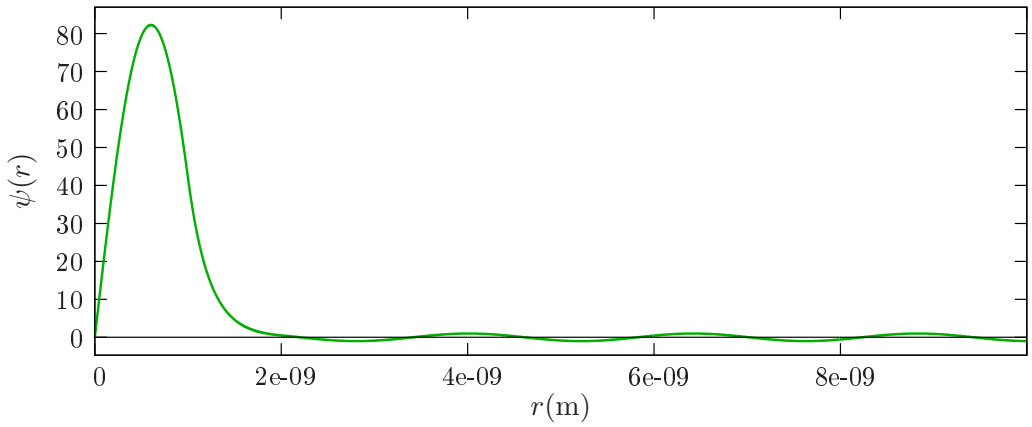

(a) $E_1 = 0.259061203092\,\text{eV}$

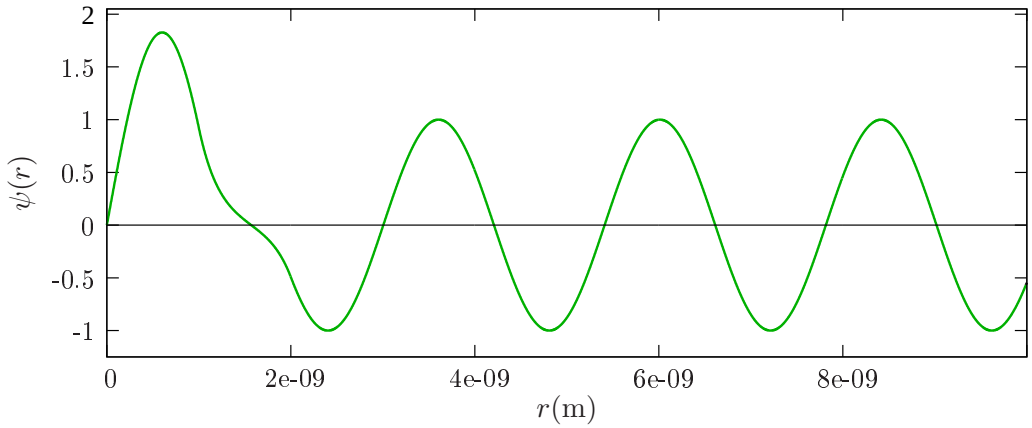

(b) $E = 0.26\,\text{eV}$

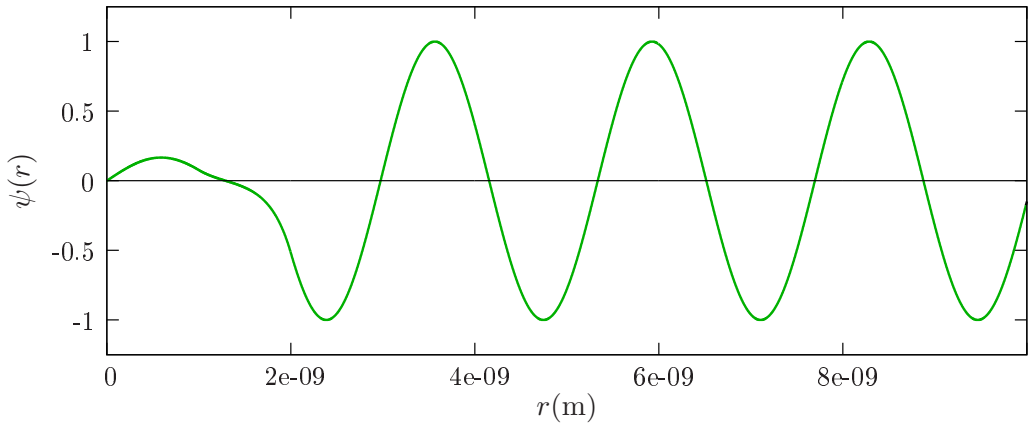

(c) $E = 0.27\,\text{eV}$

Figure 1.3: Plot of the scattered wave functions for energy $E_1 = 0.259061203092\,\text{eV}$ in the first resonance region and for energies $0.26\,\text{eV}$ and $0.27\,\text{eV}$.

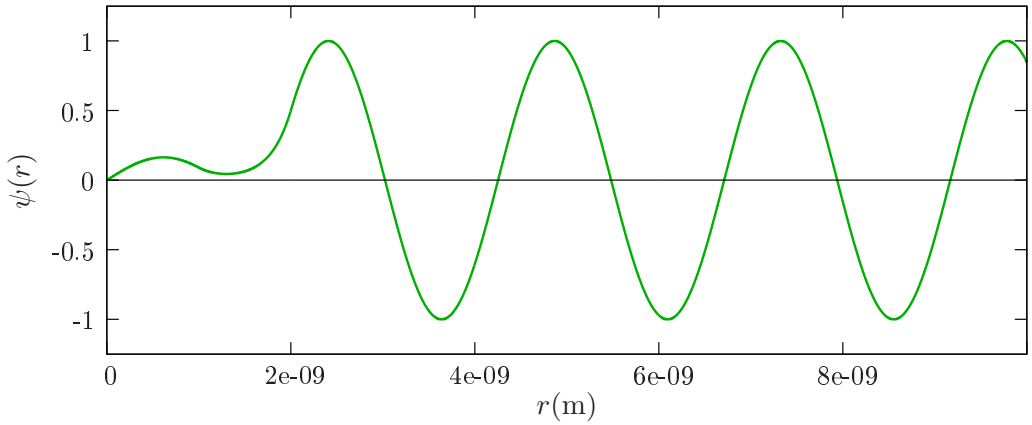

(a) $E < E_{\mathrm{res1}}$

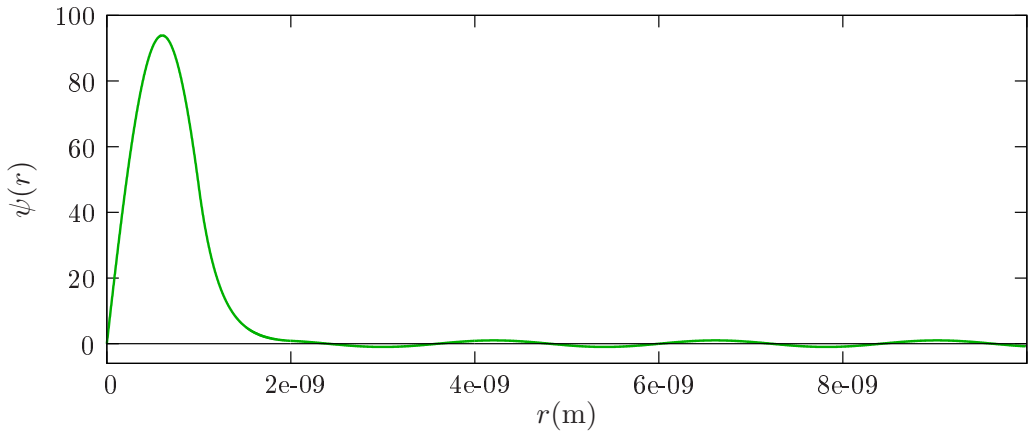

(b) $E_{\mathrm{res1}} = 0.259051096847\,\mathrm{eV}$

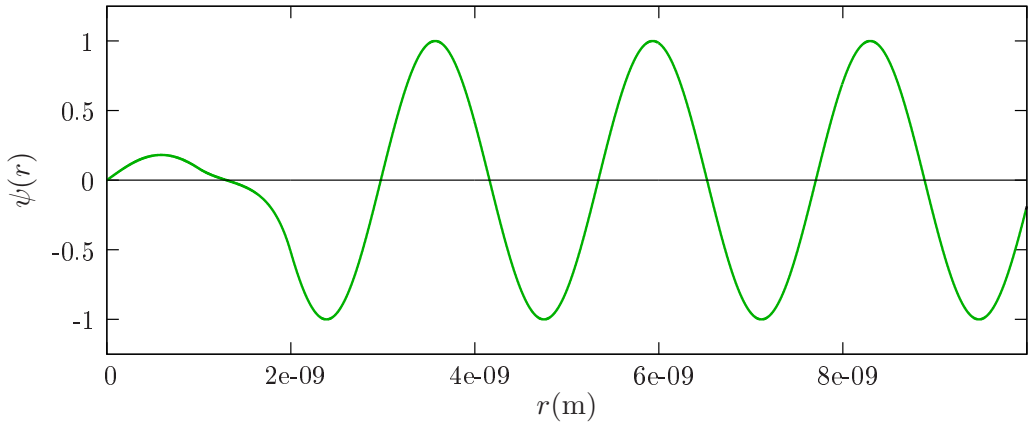

(c) $E > E_{\mathrm{res1}}$

Figure 1.4: Changes in the scattered wave functions at the first resonance $E_{\mathrm{res1}} = 0.259051096847\,\mathrm{eV}$ and for energies $E_{\mathrm{res1}} \pm 0.01\,\mathrm{eV}$ and the phase change of π as E passes through E_{res1}.

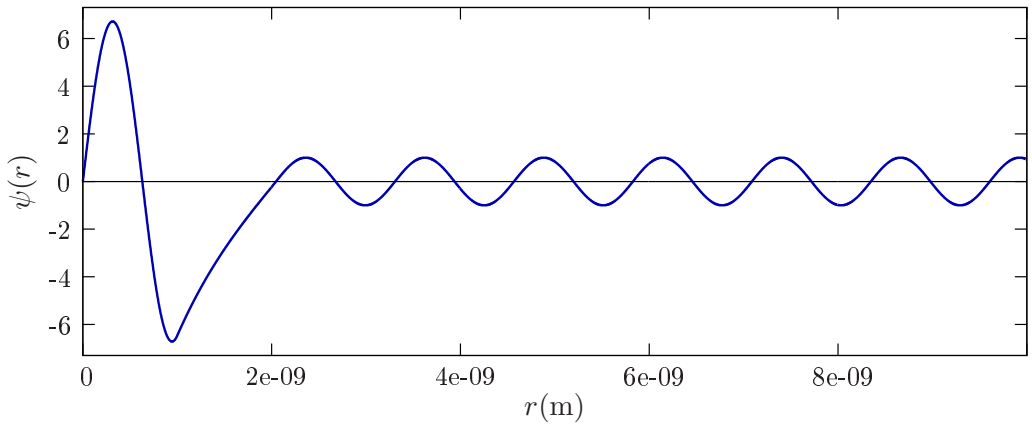

(a) $E_{\mathrm{res2}} = 0.947017018143\,\mathrm{eV}$

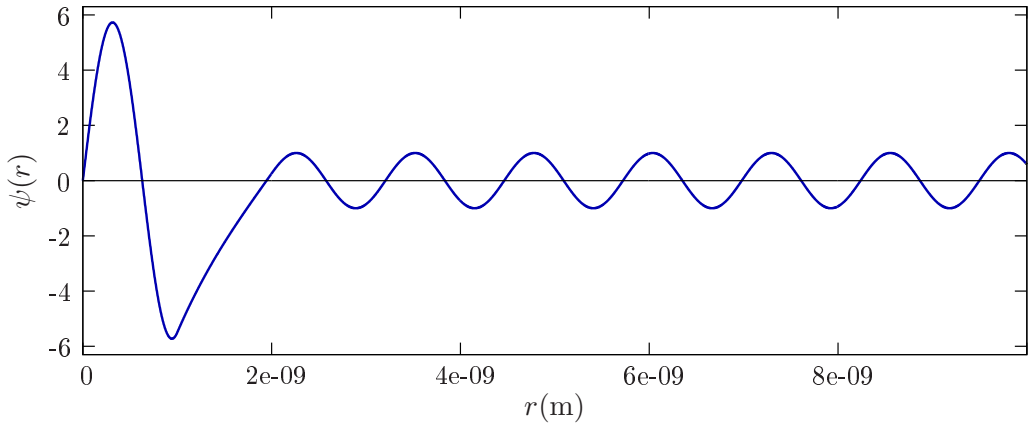

(b) $E = 0.95\,\mathrm{eV}$

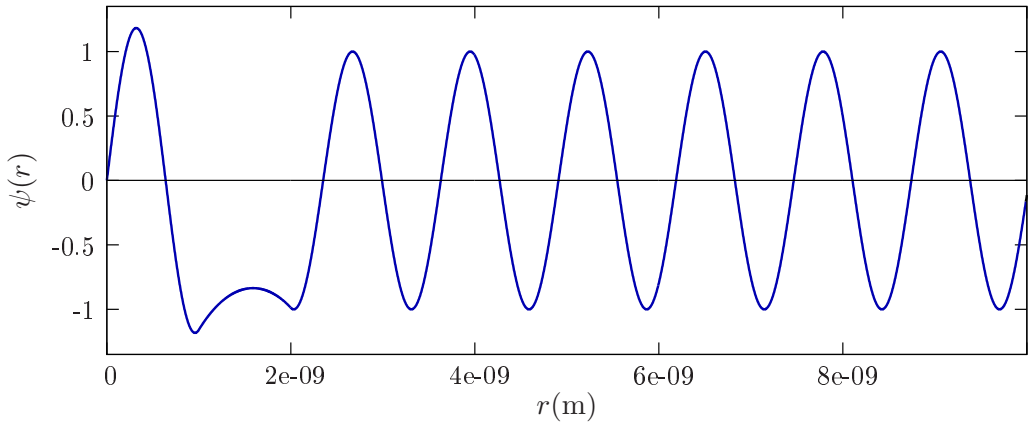

(c) $E = 0.92\,\mathrm{eV}$

Figure 1.5: Plot of the scattered wave functions for the second resonance $E_{\mathrm{res2}} = 0.947017018143\,\mathrm{eV}$ and for energies $0.95\,\mathrm{eV}$ and $0.92\,\mathrm{eV}$.

The resonance is characterized by its energy E and tunelling width $\Gamma^{\rm t}$. The lifetime of the decay and the energy is related by an approximate formula [16]

$$\tau^{\rm t} = \frac{M}{8\hbar}\frac{\kappa_0^4}{\kappa^3 k^3} e^{2\kappa(r_2-r_1)}(1+\kappa r_1)\,, \qquad \kappa_0^2 = \frac{2M(U_0-E_0)}{\hbar^2}\,, \tag{1.6}$$

where E_0 is the lowest resonance energy. The width $\Gamma^{\rm t}$ is determined from the lifetime of the state by the relation

$$\Gamma^{\rm t} = \frac{\hbar}{\tau^{\rm t}}\,. \tag{1.7}$$

Calculated values of resonance widths and lifetimes for the resonance energies via equations (1.6) and (1.7) are listed in Table 1.1.

Table 1.1: Comparison of calculated resonance widths and lifetimes.

E	$\Gamma^{\rm t}$	$\tau^{\rm t}$
$E_{\rm res1} = 0.259051096847\,{\rm eV}$	$0.000066940095\,{\rm eV}$	$9.83\times10^{-12}\,{\rm s}$
$E_{\rm res2} = 0.947017018143\,{\rm eV}$	$0.014213192312\,{\rm eV}$	$4.63\times10^{-14}\,{\rm s}$

The solution of Eq. (1.2) has the asymptotic form (*i.e.*, for $r\to\infty$) [20]

$$\psi(r) \simeq D\left[\sin(kr - L\pi/2) + \tan\delta_L \cos(kr - L\pi/2)\right], \tag{1.8}$$

where δ_L is the real scattering phase shift of the Lth partial wave induced by the potential $V(r)$. The value of $\tan\delta_L$ may be computed using the formula

$$\tan\delta_L = \frac{\psi(R_2)\sin(kR_1 - L\pi/2) - \psi(R_1)\sin(kR_2 - L\pi/2)}{\psi(R_1)\cos(kR_2 - L\pi/2) - \psi(R_2)\cos(kR_1 - L\pi/2)} \tag{1.9}$$

for R_1 and R_2 distinct points in the asymptotic region such that R_2 is the right-hand end point of the interval of integration and $R_1 = R_2 - h$ where h is the step interval. The term $L\pi/2$ in (1.8) is conventional. The numbers [5]

$$\sigma_L(E) = \frac{2\pi\hbar^2}{ME}(2L+1)\sin^2\delta_L(E)$$

are usually called partial cross sections, and the total scattering cross section $\sigma(E)$ is their sum over all L.

The partial cross sections for $L=0$ as a function of the energy for each of the quasi-bound states are displayed in Figure 1.7. The phase shift behavior for $L=0$ is indicated in Figure 1.6.

As we shall see in the third chapter the quasi-bound resonance states play a crucial role in the process of radiative association.

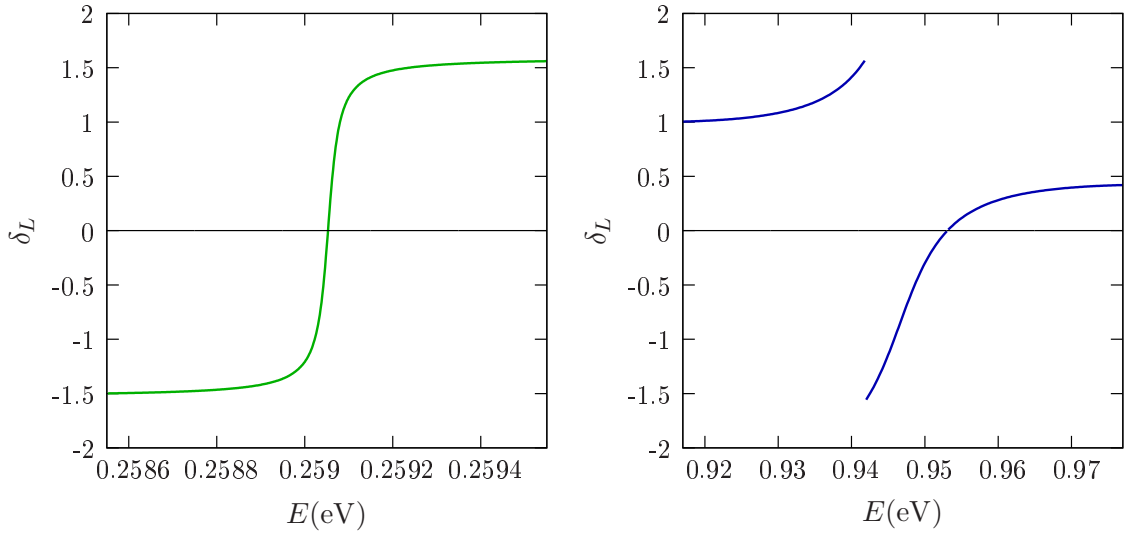

Figure 1.6: A resonant change in the phase shift for the $L = 0$ states.

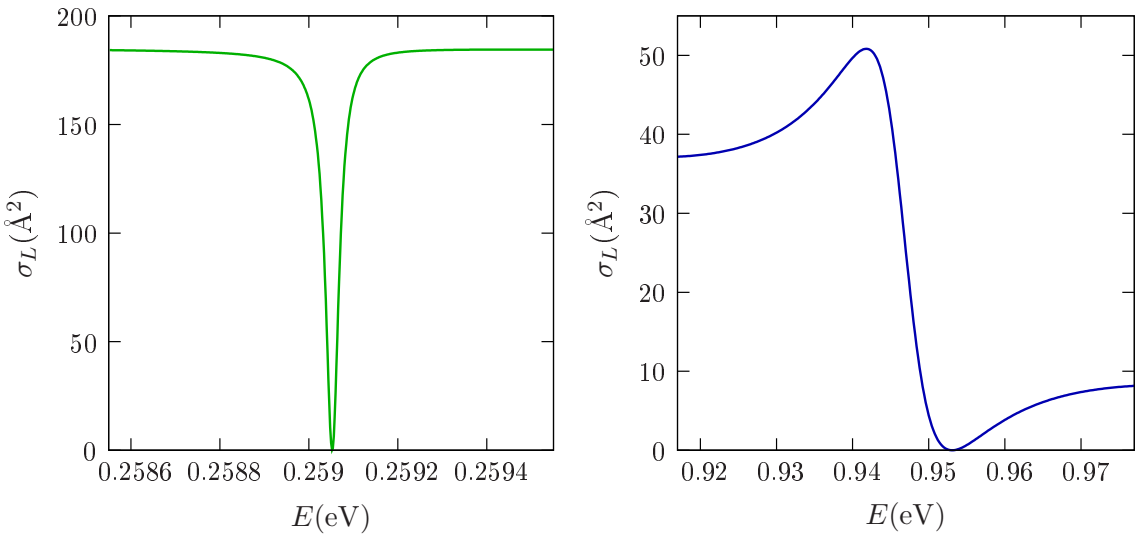

Figure 1.7: Partial ($L = 0$) cross-section resonance line shapes.

Chapter 2

Theory of electric-multipole transitions for linear molecules

2.1 Background

Let an atom/molecule be in an excited level n, that is, in a level of more than the minimum energy. Einstein then ascribes to it a certain probability per unit time, $A_{n\to m}$, of making a spontaneous transition with emission of radiation to each level m of lower energy. For electric dipole transitions, the Einstein transition probability of spontaneous emission from excited state n to lower state m is given in atomic units (in which $\hbar = e = m_e = 1$) by [6]

$$A^{\text{dip.}}_{n\to m} = \frac{64\pi^4 \tilde{\nu}^3_{n\to m}}{3h} \frac{S^{\text{dip.}}(J', J'')}{2J'+1}\,, \tag{2.1}$$

where $S^{\text{dip.}}(J', J'')$ is the line strength defined in the terms of the dipole moment and $\tilde{\nu}_{n\to m} = (E_{n,J'} - E_{m,J''})/hc$ is the wavenumber of each emitted photon. Similarly, the Einstein spontaneous quadrupole emission probability for the transition from n to m in atomic units becomes

$$A^{\text{quad.}}_{n\to m} = \frac{32\pi^6 \tilde{\nu}^5_{n\to m}}{5h} \frac{S^{\text{quad.}}(J', J'')}{2J'+1}\,,$$

where $S^{\text{quad.}}(J', J'')$ is the corresponding line strength for transition based on the quadrupole moment. Note the common convention that J' corresponds to the upper rotational quantum number of the excited state n, while J'' corresponds to that of the lower state m.

2.2 Fundamental formula for the line strengths

In this section we derive line strength formulae for Hund's case (a) linear molecules. For general discussion of Hund's cases see Ref. [4]. Throughout this chapter we will follow notation of Ref. [11]. Derivation will be performed for quadrupole moment. Generalized multipole line strength will be found through a direct analysis of the quadrupole line strength. We use capital letters for space-fixed axes and lower case letters for molecule-fixed axes. The notation for quantum number symbols will be as follows: The quantum number J corresponds to the total angular momentum of a diatomic molecule. The total angular momentum excluding the electronic spin angular momentum is represented by quantum number N.

If the spin angular momentum $\mathbf{S}$ is tightly coupled to the internuclear axis, the axial components of the electronic orbital angular momentum $\mathbf{L}$ and $\mathbf{S}$ are well defined and are assigned a quantum number Λ and Σ. Their sum is denoted Ω, *i.e.*, $\Omega = \Lambda + \Sigma$. This kind of coupling, for which J is the most appropriate quantum number to be used to describe the total angular momentum, is called Hund's case (a). When the spin vector $\mathbf{S}$ is no longer coupled to the internuclear axis, Ω is consequently not defined, and it is more appropriate to use N instead of the total angular momentum quantum number. This is Hund's case (b). These two cases are the most widely observed for diatomic molecules. For Hund's case (a) type molecules the projection of angular momentum $\mathbf{P}$ along the internuclear axis, represented by quantum number Ω, commutes with Hamiltonian of the system. In other words $\mathbf{P}$ is conserved.

The electric quadrupole moment can be written in terms of second-rank spherical tensor components $Q^{(2)}_p(\mathbf{X})$, where $\mathbf{X} = (X, Y, Z)$ are the laboratory-fixed coordinates, and $p = -2, -1, 0, 1, 2$ represents the projection quantum number of the quadrupole moment. Upon an inverse rotation to express the space coordinates (X, Y, Z) in terms of the molecular coordinates $\mathbf{x} = (x, y, z)$, in which quantum mechanical calculations are generally performed, the quadrupole moment becomes

$$Q^{(2)}_p(\mathbf{X}) = \sum_q T^{(2)*}_{pq} Q^{(2)}_q(\mathbf{x})\,, \tag{2.2}$$

where $T^{(2)*}_{pq}$ is the second-rank spherical rotation tensor in terms of the Euler angles $\omega = (\alpha\beta\gamma)$ satisfying

$$T^{(2)}_{pq}(\alpha, \beta, \gamma)^* = T^{(2)}_{qp}(-\alpha, -\beta, -\gamma)\,.$$

The symbol ω is commonly used as a short-hand for the orientation $(\alpha\beta\gamma)$. The volume element for integration is $\mathrm{d}\omega = \sin\beta\,\mathrm{d}\alpha\,\mathrm{d}\beta\,\mathrm{d}\gamma$, and $\int \mathrm{d}\omega = 8\pi^2$.

The line strength $S^{\mathrm{quad.}}(J', J'')$ for the electric-quadrupole transition between

two rovibronic states of the form

$$|\psi_i\rangle = |n', v', \Omega'; J', M', \Omega'\rangle = |n', v', \Omega'\rangle\,|J', M', \Omega'\rangle\,,$$
$$|\psi_f\rangle = |n'', v'', \Omega''; J'', M'', \Omega''\rangle = |n'', v'', \Omega''\rangle\,|J'', M'', \Omega'\rangle\,,$$

where v is the vibrational quantum number, the label n stands for the assembly of all other relevant electronic quantum numbers and M range through the $2J+1$ degeneracies, is given in the space-fixed frame by

$$S^{\text{quad.}}(J', J'') = \sum_p \sum_{M', M''} \left|\langle\psi_i|\, Q_p^{(2)}(\mathbf{X})\,|\psi_f\rangle\right|^2 .$$

To simplify the calculation, if there is no spatial preference for the laboratory-fixed quadrupole moment, we may also choose the Z-axis to be the internuclear axis. Given these assumptions the quadrupole terms reduce to five terms, in which p can be set to equal zero:

$$S^{\text{quad.}}(J', J'') = 5 \sum_{M', M''} \left|\langle\psi_i|\, Q_0^{(2)}(\mathbf{X})\,|\psi_f\rangle\right|^2 .$$

Introducing the transformation (2.2) into the above equation, we get

$$S^{\text{quad.}}(J', J'') = 5 \sum_{M', M''} \left| \sum_q \langle n', v', \Omega'|\, Q_q^{(2)}\,|n'', v'', \Omega''\rangle \langle J', M', \Omega'|\, {T_{0q}^{(2)}}^*\,|J'', M'', \Omega''\rangle \right|^2 . \tag{2.3}$$

Note that we have made use of the Born-Oppenheimer approximation which allows us to separate the vibronic $|n, v, \Omega\rangle$ and rotational $|J, M, \Omega\rangle$ wave functions.

Due to the symmetry of linear molecules along the internuclear axis, the normalized rotational wave function of a symmetric top is of the form [11]

$$\langle\alpha, \beta, \gamma|J, M, \Omega\rangle = \left(\frac{2J+1}{8\pi^2}\right)^{1/2} {\mathcal{D}^J_{M\Omega}(\alpha\beta\gamma)}^* ,$$

where ${\mathcal{D}^J_{M\Omega}}^*$ is the complex conjugate of the $M\Omega$ element of the $(2J+1)\times(2J+1)$ matrix called a Wigner rotation matrix. We now may evaluate the matrix elements of ${T_{pq}^{(2)}}^*$ as

$$\langle J', M', \Omega'|\, {T_{pq}^{(2)}}^*\,|J'', M'', \Omega''\rangle = \frac{[(2J'+1)(2J''+1)]^{1/2}}{8\pi^2} \int \mathcal{D}^{J'}_{M'\Omega'} {T_{pq}^{(2)}}^* {\mathcal{D}^{J''}_{M''\Omega''}}^* \mathrm{d}\omega\,. \tag{2.4}$$

The value of the integral in Eq. (2.4) is given as a function of Clebsch-Gordan coefficients by

$$\int \mathcal{D}^{J'}_{M'\Omega'} {T_{0q}^{(2)}}^* {\mathcal{D}^{J''}_{M''\Omega''}}^* \mathrm{d}\omega = \frac{8\pi^2}{2J'+1} \langle J', \Omega'|J'', \Omega''; 2, q\rangle \langle J', M'|J'', M''; 2, 0\rangle\,. \tag{2.5}$$

Using (2.4) and (2.5), Eq. (2.3) can be now rewritten as

$$S^{\text{quad.}}(J', J'') = 5\,\frac{2J''+1}{2J'+1}\sum_{M',M''}\left|\langle J'', M''; 2, 0|J'M'\rangle\right|^2 \times \\ \times\left|\sum_q \langle n', v', \Omega'|\, Q_q^{(2)}\,|n'', v'', \Omega''\rangle\langle J', M', \Omega'|\, T_{0q}^{(2)^*}\,|J'', M'', \Omega''\rangle\right|^2 .$$

If we now rewrite $\langle J'', M''; 2, 0|J'M'\rangle$ through the identity [12]

$$\langle j_1, m_1; j_2, m_2|J, M\rangle = (-1)^{j_1-m_1}\left(\frac{2J+1}{2j_2+1}\right)^{1/2}\langle j_1, m_1; J, -M|j_2, -m_2\rangle$$

and apply the sum rule property (2.7) on the term $\sum_{M',M''}|\langle J'', M''; J', -M'|2, 0\rangle|^2$, then the line strength reduces to

$$S^{\text{quad.}}(J', J'') = (2J''+1)\left|\sum_q \langle n', v', \Omega'|\, Q_q^{(2)}\,|n'', v'', \Omega''\rangle\langle J', M', \Omega'|\, T_{0q}^{(2)^*}\,|J'', M'', \Omega''\rangle\right|^2 .$$

The summation over $q = \Omega' - \Omega'' = \triangle\Omega$ is redundant, because only one value for q is defined by the transition being considered, namely

$$S^{\text{quad.}}(J', J'') = \left|\langle n', v', \Omega'|\, Q^{(2)}\,|n'', v'', \Omega''\rangle\right|^2 (2J''+1)\,\left|\langle J'', \Omega''; 2, \triangle\Omega|J', \Omega'\rangle\right|^2 ,$$

for $\triangle\Omega = -2, -1, 0, 1, 2$ and for $\triangle J = J' - J'' = -2, -1, 0, 1, 2$ (the O, P, Q, R, S branches). Accordingly, for a dipole moment

$$S^{\text{dip.}}(J', J'') = \left|\langle n', v', \Omega'|\, Q^{(1)}\,|n'', v'', \Omega''\rangle\right|^2 (2J''+1)\,\left|\langle J'', \Omega''; 1, \triangle\Omega|J', \Omega'\rangle\right|^2 ,$$

for $\triangle\Omega = -1, 0, 1$ and for $\triangle J = J' - J'' = -1, 0, 1$ (the P, Q, R branches). The general multipole line strength formula for an allowed rovibronic transition can be calculated through the same procedure to obtain

$$S^{l-\text{pole}}(J', J'') = \left|M^{(l)}_{n',v',\Omega';n'',v'',\Omega''}\right|^2 \mathscr{S}^{l-\text{pole}}(J', J'')$$

where the vibronic transition moment is given by

$$M^{(l)}_{n',v',\Omega';n'',v'',\Omega''} = \langle n', v', \Omega'|\, Q^{(l)}\,|n'', v'', \Omega''\rangle \tag{2.6}$$

and the quantity representing a rotational part of the line strength is called the Hönl-London factor

$$\mathscr{S}^{l-\text{pole}}(J', J'') = (2J''+1)\,\left|\langle J'', \Omega''; l, \triangle\Omega|J', \Omega'\rangle\right|^2 .$$

for $\triangle\Omega = -l, -l+1, \ldots, l-1, l$ and for $\triangle J = J' - J'' = -l, -l+1, \ldots, l-1, l$. Explicit expressions for the Hönl-London factors of dipole and quadrupole moment are given in Tables 2.1 and 2.2.

Finally, we separate off the electronic motion by invoking the Born-Oppenheimer approximation, when the electronic wave function is obtained on the assumption that the nuclei are at a fixed separation R, by writing the vibronic wave function as a product $|n, v, \Omega\rangle = \psi_{n,\Omega}(r_e; R)\psi_v(R)$. Therefore, the matrix element of the transition moment (2.6) can be written as

$$M^{(l)}_{v',v''} = \int_0^\infty \psi_{v'}(R)\, Q^{(l)}(R)\, \psi_{v''}(R)\, \mathrm{dR}\,.$$

Table 2.1: Hönl-London factors for electric dipole transitions of linear Hund's case (a) molecules.

$\mathscr{S}^{\mathrm{dip.}}(J', J'')$	$\triangle J = -1$ P-branch	$\triangle J = 0$ Q-branch	$\triangle J = +1$ R-branch
$\triangle\Omega = -1$	$\frac{(J'+\Omega'+1)(J'+\Omega'+2)}{2(J'+1)}$	$\frac{(2J'+1)(J'-\Omega')(J'+\Omega'+1)}{2J'(J'+1)}$	$\frac{(J'-\Omega'-1)(J'-\Omega')}{2J'}$
$\triangle\Omega = 0$	$\frac{(J'-\Omega'+1)(J'+\Omega'+1)}{J'+1}$	$\frac{\Omega'^2(2J'+1)}{J'(J'+1)}$	$\frac{(J'-\Omega')(J'+\Omega')}{J'}$
$\triangle\Omega = +1$	$\frac{(J'-\Omega'+1)(J'-\Omega'+2)}{2(J'+1)}$	$\frac{(2J'+1)(J'+\Omega')(J'-\Omega'+1)}{2J'(J'+1)}$	$\frac{(J'+\Omega'-1)(J'+\Omega')}{2J'}$

Table 2.2: Hönl-London factors for electric quadrupole transitions of linear Hund's case (a) molecules.

$\mathscr{S}^{\text{quad.}}(J', J'')$	$\triangle J = -1$ P-branch	$\triangle J = 0$ Q-branch	$\triangle J = +1$ R-branch
$\triangle\Omega = -2$	$\frac{(J'-\Omega')(J'+\Omega'+1)(J'+\Omega'+2)(J'+\Omega'+3)}{2J'(J'+1)(J'+2)}$	$\frac{3(2J'+1)(J'-\Omega'-1)(J'-\Omega')(J'+\Omega'+1)(J'+\Omega'+2)}{(2J'-1)2J'(J'+1)(2J'+3)}$	$\frac{(J'-\Omega'-2)(J'-\Omega'-1)(J'-\Omega')(J'+\Omega'+1)}{2(J'-1)J'(J'+1)}$
$\triangle\Omega = -1$	$\frac{(J'-2\Omega')^2(J'+\Omega'+1)(J'+\Omega'+2)}{2J'(J'+1)(J'+2)}$	$\frac{3(2J'+1)(2\Omega'+1)^2(J'-\Omega')(J'+\Omega'+1)}{2(2J'-1)J'(J'+1)(2J'+3)}$	$\frac{(J'+2\Omega'+1)^2(J'-\Omega'-1)(J'-\Omega')}{2(J'-1)J'(J'+1)}$
$\triangle\Omega = 0$	$\frac{3\Omega'^2(J'-\Omega'+1)(J'+\Omega'+1)}{J'(J'+1)(J'+2)}$	$\frac{(2J'+1)(3\Omega'^2-J'(J'+1))^2}{J'(J'+1)(2J'-1)(2J'+3)}$	$\frac{3\Omega'^2(J'-\Omega')(J'+\Omega')}{(J'-1)J'(J'+1)}$
$\triangle\Omega = +1$	$\frac{(J'+2\Omega')^2(J'-\Omega'+1)(J'-\Omega'+2)}{2J'(J'+1)(J'+2)}$	$\frac{3(2J'+1)(2\Omega'-1)^2(J'+\Omega')(J'-\Omega'+1)}{2(2J'-1)J'(J'+1)(2J'+3)}$	$\frac{(J'-2\Omega'+1)^2(J'+\Omega'-1)(J'+\Omega')}{2(J'-1)J'(J'+1)}$
$\triangle\Omega = +2$	$\frac{(J'+\Omega')(J'-\Omega'+1)(J'-\Omega'+2)(J'-\Omega'+3)}{2J'(J'+1)(J'+2)}$	$\frac{3(2J'+1)(J'+\Omega'-1)(J'+\Omega')(J'-\Omega'+1)(J'-\Omega'+2)}{(2J'-1)2J'(J'+1)(2J'+3)}$	$\frac{(J'+\Omega'-2)(J'+\Omega'-1)(J'+\Omega')(J'-\Omega'+1)}{2(J'-1)J'(J'+1)}$

$\mathscr{S}^{\text{quad.}}(J', J'')$	$\triangle J = -2$ O-branch	$\triangle J = +2$ S-branch
$\triangle\Omega = -2$	$\frac{(J'+\Omega'+1)(J'+\Omega'+2)(J'+\Omega'+3)(J'+\Omega'+4)}{4(J'+1)(J'+2)(2J'+3)}$	$\frac{(J'-\Omega'-3)(J'-\Omega'-2)(J'-\Omega'-1)(J'-\Omega')}{4J'(J'-1)(2J'-1)}$
$\triangle\Omega = -1$	$\frac{(J'-\Omega'+1)(J'+\Omega'+1)(J'+\Omega'+2)(J'+\Omega'+3)}{(J'+1)(J'+2)(2J'+3)}$	$\frac{(J'-\Omega'-2)(J'-\Omega'-1)(J'-\Omega')(J'+\Omega')}{J'(J'-1)(2J'-1)}$
$\triangle\Omega = 0$	$\frac{3(J'-\Omega'+1)(J'-\Omega'+2)(J'+\Omega'+1)(J'+\Omega'+2)}{2(J'+1)(J'+2)(2J'+3)}$	$\frac{3(J'-\Omega'-1)(J'-\Omega')(J'+\Omega'-1)(J'+\Omega')}{2J'(J'-1)(2J'-1)}$
$\triangle\Omega = +1$	$\frac{(J'-\Omega'+1)(J'-\Omega'+2)(J'-\Omega'+3)(J'+\Omega'+1)}{(J'+1)(J'+2)(2J'+3)}$	$\frac{(J'-\Omega')(J'+\Omega')(J'+\Omega'-1)(J'+\Omega'-2)}{J'(J'-1)(2J'-1)}$
$\triangle\Omega = +2$	$\frac{(J'-\Omega'+1)(J'-\Omega'+2)(J'-\Omega'+3)(J'-\Omega'+4)}{4(J'+1)(J'+2)(2J'+3)}$	$\frac{(J'+\Omega'-3)(J'+\Omega'-2)(J'+\Omega'-1)(J'+\Omega')}{4J'(J'-1)(2J'-1)}$

2.3 Appendix: Coupling of angular momenta

The coupling of two angular momenta $\mathbf{J}_1$ and $\mathbf{J}_2$ to form a resultant one, $\mathbf{J} = \mathbf{J}_1 + \mathbf{J}_2$, is familiar to all physicists. It is supposed that $\mathbf{J}_1$ and $\mathbf{J}_2$ act on different physical systems, or else on independent parts of the same system. This guarantees that $\mathbf{J}_1$ and $\mathbf{J}_2$ commute, thereby ensuring that the components of $\mathbf{J}$ obey the standard commutation relations. We can describe the combined system by two types of ket. We can choose either the uncoupled states $|j_1, m_1\rangle\,|j_2, m_2\rangle$, or the coupled states $|j, m, j_1, j_2\rangle$. For a given j_1 and j_2, the tensor product of the vector space spanned by the states $|j_1, m_1\rangle$, $m_1 = -j_1, \ldots, j_1$ and of the vector space spanned by $|j_2, m_2\rangle$, $m_2 = -j_2, \ldots, j_2$ has a $(2j_1+1)(2j_2+1)$ dimensional uncoupled basis $|j_1, m_1\rangle\,|j_2, m_2\rangle$. If we use the fact that j can run with integer step from $j_1 + j_2$ down to $|j_1 - j_2|$, there is an equal number of coupled kets as $\sum_{j=|j_1-j_2|}^{j_1+j_2}(2j+1) = (2j_1+1)(2j_2+1)$. The unitary transformation that connects the two descriptions can be written in the general form:

$$|j, m, j_1, j_2\rangle = \sum_{m_1, m_2} |j_1, m_1\rangle\,|j_2, m_2\rangle\,\langle j_1, j_2, m_1, m_2|j, m\rangle\,.$$

The coefficients $\langle j_1, j_2, m_1, m_2|j, m\rangle$ are the celebrated Clebsch-Gordan angular momentum coupling coefficients. Phases can be chosen so that they are all real. The total angular momentum states satisfy the orthogonality relations:

$$\sum_{j,m} \langle j_1, m_1, j_2, m_2|j, m\rangle\,\langle j, m|j_1, m_1', j_2, m_2'\rangle = \delta_{m_1,m_1'}\delta_{m_2,m_2'}\,,$$

$$\sum_{m_1,m_2} \langle j, m|j_1, m_1, j_2, m_2\rangle\,\langle j_1, m_1, j_2, m_2|j', m'\rangle = \delta_{j,j'}\delta_{m,m'}\,. \tag{2.7}$$

The Clebsch-Gordan coefficients are often replaced by the Wigner 3-j symbols, defined as

$$\begin{pmatrix} j_1 & j_2 & j_3 \\ m_1 & m_2 & m_3 \end{pmatrix} = (-1)^{j_1-j_2-m_3}(2j_3+1)^{-1/2}\,\langle j_1, m_1, j_2, m_2|j_3, -m_3\rangle\,.$$

They exhibit symmetry relations of the Clebsch-Gordan coefficients in a more convenient way. The 3-j symbol is invariant under an even or cyclic permutation in the order of its columns

$$\begin{pmatrix} j_1 & j_2 & j_3 \\ m_1 & m_2 & m_3 \end{pmatrix} = \begin{pmatrix} j_2 & j_3 & j_1 \\ m_2 & m_3 & m_1 \end{pmatrix} = \begin{pmatrix} j_3 & j_1 & j_2 \\ m_3 & m_1 & m_2 \end{pmatrix},$$

while odd permutation of the columns multiplies the 3-j symbol by the phase factor $(-1)^{j_1+j_2+j_3}$

$$\begin{pmatrix} j_1 & j_2 & j_3 \\ m_1 & m_2 & m_3 \end{pmatrix} = (-1)^{j_1+j_2+j_3} \begin{pmatrix} j_2 & j_1 & j_3 \\ m_2 & m_1 & m_3 \end{pmatrix},$$

as does a reversal in sign of the entries of the lower row

$$\begin{pmatrix} j_1 & j_2 & j_3 \\ -m_1 & -m_2 & -m_3 \end{pmatrix} = (-1)^{j_1+j_2+j_3} \begin{pmatrix} j_1 & j_2 & j_3 \\ m_1 & m_2 & m_3 \end{pmatrix}.$$

Over the years, explicit algebraic formulae for the 3-j symbols have been calculated. The simplest of these formulae can be found tabulated in several texts, *e.g.* [4, 10].

Chapter 3

Radiative association of $LiHe^+$

3.1 Theory and numerical methods

In this section we study quantum mechanically the direct radiative association process

$$\mathrm{Li}^+(1s^2) \,+\, \mathrm{He}\,(1s^2) \,\rightarrow\, \mathrm{LiHe}^+(X\,{}^1\Sigma^+) \,+\, h\nu\,. \tag{3.1}$$

One-dimensional radial Schrödinger equations associated with the molecular formation (3.1), in such case radiative transition from an initial electronic state to another final electronic state, are of the form

$$\left[-\frac{\hbar^2}{2\mu}\frac{\mathrm{d}^2}{\mathrm{d}R^2} + V_J(R)\right]\psi(R) = E\,\psi(R) \tag{3.2}$$

with an effective potential

$$V_J(R) = \frac{\hbar^2}{2\mu}\frac{J(J+1)}{R^2} + U(R)\,.$$

Here $U(R)$ is a rotationless potential with a short-range repulsion and a long-range attraction with the leading asymptotic term $-C_4/R^4$ in the case of molecular ion in an electronic state Σ. That is, $U(R) \rightarrow 0$ faster than the term $J(J+1)/R^2$ so the latter is the dominant term for sufficiently large values of R. μ denotes "charge-modified reduced mass" [24] of the molecular ion with charge Q, $\mu = (m_A\,m_B)/(m_A + m_B - m_e\,Q)$, where m_A and m_B are the atomic masses of the two atoms, m_e is the electron mass. The wave function satisfies the boundary condition $\psi(0) = 0$. In the so-called asymptotic region, where the potential $U(R)$ is negligible, Eq. (3.2) is effectively reduced, in atomic units, to

$$\left[-\frac{\mathrm{d}^2}{\mathrm{d}R^2} + \frac{J(J+1)}{R^2}\right]\psi(R) = k^2\,\psi(R) \quad \text{for } R \rightarrow \infty\,,$$

where $k^2 = 2\mu E$.

The radial wave functions $\psi = \chi_{J'}$ for $E > 0$ and $\psi = \psi_{v'',J''}$ for $E < 0$ are obtained as eigenfunctions of the Schrödinger equation (3.2) with a potential curve $V'_{J'}(R)$ for an initial electronic state and $V''_{J''}(R)$ for a final electronic state, respectively. In our one-state process $X \to X$ the above pair of Schrödinger equations simplifies to a single one from which the radial wave functions are obtained. At sufficiently large distances the function $\chi_{J'}$ may be normalized to a delta function of energy $\delta(E - E')$ and so that it has the following asymptotic form [5]

$$\chi_{J'}(E,R) \simeq \left(\frac{2\mu}{\pi k}\right)^{1/2} \sin(kR - J'\pi/2 + \delta_{J'}(E)) \quad \text{for } R \to \infty\,,$$

where $\delta_{J'}(E)$ is the phase shift.

The quantum-mechanical radiative association cross section, summed over allowed transitions between a continuum state with a positive energy E and relative orbital angular momentum J' to bound states with vibrational quantum number v'', is given, in atomic units, by [14, 15]

$$\sigma(E) = \sum_{J',v'',J''} \sigma_{J',v'',J''}(E)\,, \tag{3.3}$$

where

$$\sigma_{J';v'',J''}(E) = \frac{64}{3}\frac{\pi^5}{c^3\,k^2}\,p\,\nu^3_{E;v'',J''}\,\mathscr{S}^{\rm dip.}_{J',J''}\,M^2_{E,J';v'',J''}\,. \tag{3.4}$$

In Eq. (3.4) ν is the emitted photon frequency which is equal to $(E - E_{v'',J''} + \Delta E)/h$, where E is the initial energy of relative motion, $E_{v'',J''}$ is the binding energy of vibration-rotation level $[v'', J'']$ and $\Delta E = \lim_{R\to\infty} V'(R) - \lim_{R\to\infty} V''(R)$ (see Fig. 3.1). Obviously for one-state reaction $\Delta E = 0$.

$$M_{E,J';v'',J''} = \int_0^\infty \chi_{J'}(E,R)\,Q^{(1)}(R)\,\psi_{v'',J''}(R)\,{\rm dR}$$

is the matrix element of the transition dipole moment between the initial energy-normalized continuum wave function $\chi_{J'}(E,R)$ for the partial wave J' and the final bound-state wave function $\psi_{v'',J''}(R)$. The wave functions $\chi_{J'}$ and $\psi_{v'',J''}$ were calculated by numerical integration of the radial Schrödinger equation using the Numerov-Cooley method [7], which was depicted in details in [1]. p is the probability of approach the fraction of collisions in the initial electronic state. For $\mathrm{Li}^+(1s^2)$ + $\mathrm{He}(1s^2)$, $p = 1$.

For electronic transitions with $\triangle\Omega = 0$ (e. g., between two Σ-states) governed by dipole moment we have the rotational selection rules $\triangle J = J' - J'' = \mp 1$, thus

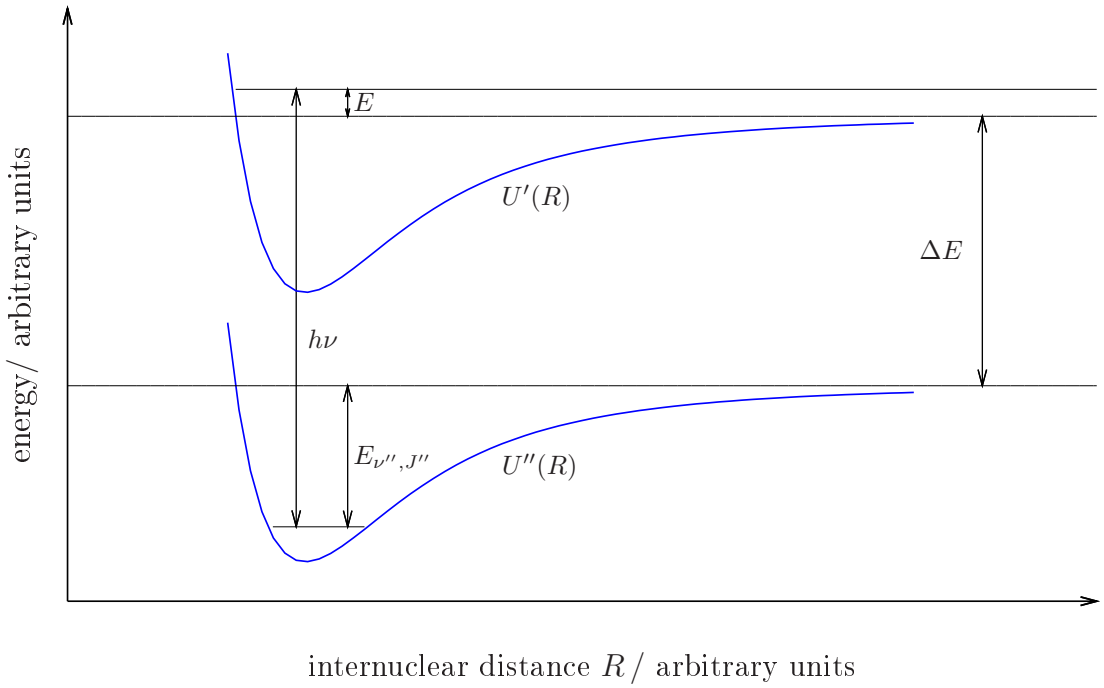

Figure 3.1: Schematic figure of the molecular transition between a continuum state with energy E supported by $U'(R)$ and a vibrational-rotational bound state with energy $E_{v'',J''}$ supported by $U''(R)$.

there are just only P and R branches. The corresponding Hönl-London coefficients read as

$$\begin{aligned} \mathscr{S}(J', J'') &= J' + 1 \quad \text{for } P\text{-branch}, \\ \mathscr{S}(J', J'') &= J' \qquad \text{for } R\text{-branch} \end{aligned}$$

for the $X\,^1\Sigma^+ \to X\,^1\Sigma^+$ dipole moment transition.

Total cross section $\sigma(E)$ for this process at a given collision energy E can be decomposed as

$$\sigma(E) = \sum_{J'} \sigma(E, J')\,,$$

where each partial cross section $\sigma(E, J')$ may be expressed as [3]

$$\sigma(E, J') = \frac{\pi}{k^2}\, p\, (2J' + 1) \mathcal{P}(E, J')$$

and

$$\mathcal{P}(E,J') = \frac{64}{3}\frac{\pi^4}{c^3}\sum_{v''}\left[\nu^3_{E;v'',J'+1}\,\frac{J'+1}{2J'+1}\,M_{v'',J'+1}(E,J')^2 + \right. \tag{3.5}$$

$$\left. + \,\nu^3_{E;v'',J'-1}\,\frac{J'}{2J'+1}\,M_{v'',J'-1}(E,J')^2\right] \tag{3.6}$$

is the opacity for this collision.

The corresponding expression in Eq. (3.3) may be rewritten by [14] as well as follows:

$$\sigma(E) = \sum_{v''=0}^{v''_{\max}}\left[\frac{64}{3}\frac{\pi^5}{c^3\,k^2}\,p\sum_{J'=0}^{\hat{J}''-1}\nu^3_{E;v'',J'+1}(J'+1)\,M_{v'',J'+1}(E,J')^2 + \right. \tag{3.7}$$

$$\left. + \sum_{J'=1}^{\hat{J}''+1}\nu^3_{E;v'',J'-1}J'\,M_{v'',J'-1}(E,J')^2\right] = \sum_{v''=0}^{v''_{\max}}\sigma_{v''}(E)\,. \tag{3.8}$$

Expression in the angular bracket reflects the partial cross section $\sigma_{v''}(E)$ associated to each final vibrational state v'' and the rotational index changes over all possible values up to $\hat{J}''-1$ for the P-branch ($J''=J'+1$) and up to $\hat{J}''+1$ for the R-branch ($J''=J'-1$). The notation $\hat{J}''=\hat{J}''(v'')$ means the largest possible value for the rotational quantum number in the final vibrational state v''.

The probability of the transition, in this case photon emission, is taken to be $\Gamma^{\rm rad}$ per unit time. The radiative width of a quasi-bound level can be written by [3]

$$\Gamma^{\rm rad}_{v',J'} = \hbar[A_P(v',J') + A_R(v',J')]\,,$$

where

$$A_P(v',J') = \sum_{v''}A_{v',J';v'',J'+1}\,,$$

$$A_R(v',J') = \sum_{v''}A_{v',J';v'',J'-1}$$

give the total spontaneous radiative decay rates via transitions with $\triangle J = \mp 1$, respectively. As noted in Chapter 2, equation (2.1), the Einstein A-coefficient for spontaneous dipole transition between a quasi-bound level $[v',J']$ and a bound vibrational-rotational level $[v'',J'']$ reads

$$A_{v',J';v'',J''} = \frac{32}{3}\frac{\pi^3}{c^3}\,\nu^3_{v',J';v'',J''}\,\mathscr{S}_{J',J''}\,M^2_{v',J';v'',J''}\,.$$

The phase shifts $\delta_{J'}$ for each J' are obtained from the asymptotic behaviour of the wave function $\chi_{J'}(R)\propto\sin(kR-J'\pi/2+\delta_{J'})$, using the algorithm of (1.9).

3.2 Results

In Table 3.1 the vibrational and rotational quantum numbers, v and J, are tabulated alongside the corresponding eigenenergies $E_{v,J}$. Energies and tunnelling widths were calculated using the computer program LEVEL 7.7 of Le Roy [17, 18].

In Table 3.2 widths and radiative lifetimes for the quasi-bound resonant states are collected. The two resonances with the narrowest tunnelling widths, $[0, 18]$ and $[1, 15]$, have radiative lifetimes significantly shorter than tunnelling lifetimes.

The potential and dipole-moment interpolation subroutines were provided by P. Soldán [21]. The potential energy curve of the $X\,^1\Sigma^+$ ground state for the process (3.1) is shown in Fig. 3.2. The zero of energy is set at the dissociation limit.

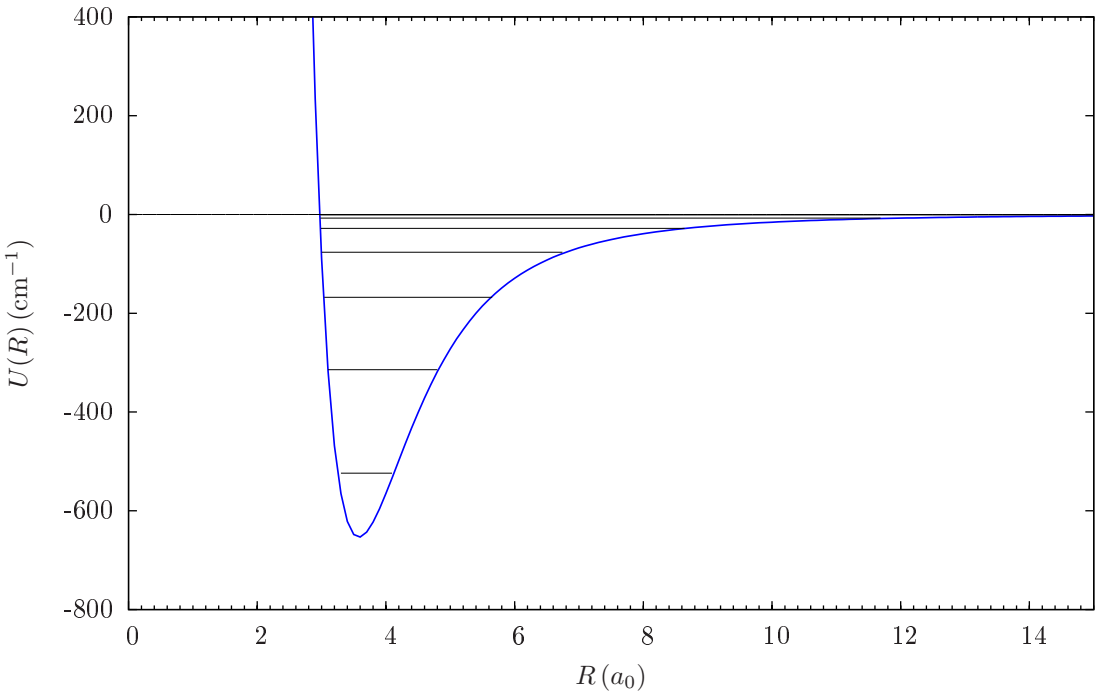

Figure 3.2: Plot of the potential of the molecular ion $LiHe^+$ in the ground electronic state $X\,^1\Sigma^+$ with its 7 bound states for $J'' = 0$.

The radiative widths, phase shifts, scattering cross sections, and cross sections for radiative association were calculated by making use of our own computer codes [2]. The integration for the continuum wave function was carried out over the range from $R = 1.2\,\mathrm{a_0}$ to $R = 1001.2\,\mathrm{a_0}$. The masses of the two atomic species are taken to have the values $m\,(^4\mathrm{He}) = 4.00260324\,\mathrm{u}$ and $m\,(^7\mathrm{Li}) = 7.0160030\,\mathrm{u}$.

Table 3.1: Bound states and resonances of the molecular ion $LiHe^+$ ($X\,^1\Sigma^+$). Energy units are cm^{-1}, and $E = 0$ at dissociation. Energies and tunnelling widths were calculated using LEVEL 7.7 [17, 18].

v	J	$E_{v,J}$	$\Gamma^{t}_{v,J}$	v	J	$E_{v,J}$	$\Gamma^{t}_{v,J}$	v	J	$E_{v,J}$	$\Gamma^{t}_{v,J}$
0	0	−523.828665		1	7	−234.441164		3	3	−66.395977	
0	1	−520.391051		1	8	−212.245308		3	4	−59.794594	
0	2	−513.524705		1	9	−187.612449		3	5	−51.721341	
0	3	−503.247477		1	10	−160.679082		3	6	−42.309086	
0	4	−489.586357		1	11	−131.610006		3	7	−31.735443	
0	5	−472.577750		1	12	−100.606469		3	8	−20.241375	
0	6	−452.267856		1	13	−67.919463		3	9	−8.170520	
0	7	−428.713194		1	14	−33.873500		3	10	3.915842	$0.430140E{-}04$
0	8	−401.981289		1	15	1.084363	$0.333273E{-}25$	3	11	14.834581	1.159244
0	9	−372.151568		1	16	36.250312	$0.563019E{-}03$	4	0	−28.192923	
0	10	−339.316551		1	17	70.058604	0.707783	4	1	−27.077585	
0	11	−303.583420		2	0	−167.663356		4	2	−24.876259	
0	12	−265.076136		2	1	−165.343526		4	3	−21.649754	
0	13	−223.938361		2	2	−160.719722		4	4	−17.495260	
0	14	−180.337616		2	3	−153.824092		4	5	−12.556094	
0	15	−134.471430		2	4	−144.705984		4	6	−7.042051	
0	16	−86.576987		2	5	−133.433459		4	7	−1.282597	
0	17	−36.947430		2	6	−120.095584		4	8	4.012297	0.257264
0	18	14.037107	$0.496631E{-}15$	2	7	−104.805871		5	0	−7.410469	
0	19	65.837039	$0.417492E{-}04$	2	8	−87.707479		5	1	−6.800953	
0	20	117.475804	$0.936215E{-}01$	2	9	−68.981371		5	2	−5.620133	
0	21	167.328071	2.959228	2	10	−48.859876		5	3	−3.950100	
1	0	−314.221174		2	11	−27.651455		5	4	−1.933488	
1	1	−311.318136		2	12	−5.793621		5	5	0.164320	$0.546609E{-}04$
1	2	−305.523666		2	13	15.987916	$0.117041E{-}02$	6	0	−0.980784	
1	3	−296.861167		2	14	36.109853	1.476570	6	1	−0.748464	
1	4	−285.366233		3	0	−76.525097		6	2	−0.335863	
1	5	−271.087293		3	1	−74.818489		6	3	0.109688	$0.445954E{-}01$
1	6	−254.086525		3	2	−71.427187		7	0	−0.010756	

Table 3.2: Quasi-bound resonance states, tunnelling widths $\Gamma^{\rm t}_{v',J'}$, radiative widths $\Gamma^{\rm rad}_{v',J'}$ and the corresponding lifetimes $\tau^{\rm t}_{v',J'}$, $\tau^{\rm rad}_{v',J'}$ of the molecular ion $LiHe^+$ ($X\,^1\Sigma^+$). Energy units are cm^{-1}. Lifetimes are given in s.

v'	J'	E	$\Gamma^{\rm t}_{v',J'}$	$\Gamma^{\rm rad}_{v',J'}$	$\tau^{\rm t}_{v',J'}$	$\tau^{\rm rad}_{v',J'}$
0	18	14.037107	$0.496631E{-}15$	$0.192826E{+}07$	$0.106897E{+}05$	$0.275317E{-}17$
0	19	65.837039	$0.417492E{-}04$	0	$0.127162E{-}06$	–
0	20	117.475804	$0.936215E{-}01$	0	$0.567054E{-}10$	–
0	21	167.328071	2.959228	0	$0.179399E{-}11$	–
1	15	1.084363	$0.333273E{-}25$	$0.100601E{+}18$	$0.159294E{+}15$	$0.527711E{-}28$
1	16	36.250312	$0.563019E{-}03$	$0.518663E{-}06$	$0.942923E{-}08$	$0.102356E{-}04$
1	17	70.058604	0.707783	$0.649969E{-}05$	$0.750066E{-}11$	$0.816783E{-}06$
2	13	15.987916	$0.117041E{-}02$	$0.386258E{-}05$	$0.453589E{-}08$	$0.137443E{-}05$
2	14	36.109853	1.476570	$0.998735E{-}05$	$0.359539E{-}11$	$0.531556E{-}06$
3	10	3.915842	$0.430140E{-}04$	$0.218746E{-}06$	$0.123421E{-}06$	$0.242694E{-}04$
3	11	14.834581	1.159244	$0.105469E{-}04$	$0.457957E{-}11$	$0.503358E{-}06$
4	8	4.012297	0.257264	$0.190346E{-}04$	$0.206358E{-}10$	$0.278904E{-}06$
5	5	0.164320	$0.546609E{-}04$	$0.728781E{-}06$	$0.971231E{-}07$	$0.728454E{-}05$
6	3	0.109688	$0.445954E{-}01$	$0.261698E{-}05$	$0.119045E{-}09$	$0.202861E{-}05$

3.2.1 Phase shifts and cross sections for resonances of the molecular ion $LiHe^+$

In the first stage we have calculated the phase shifts and the partial scattering cross sections in the vicinity of resonance energies in order to verify the results of LEVEL 7.7. Figures for the very narrow resonances, $[0, 18]$ and $[1, 15]$, are not listed as they are not resolved within the 16 digit accuracy.

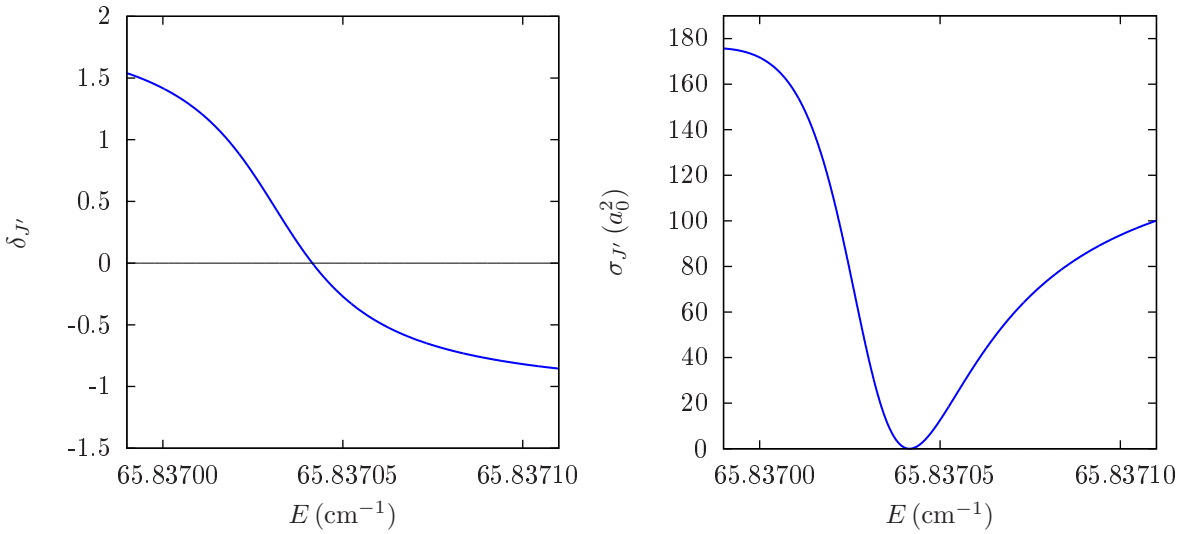

Figure 3.3: Computed phase shift and partial ($J' = 19$) scattering cross section resonance line shape on vibrational manifold $v' = 0$.

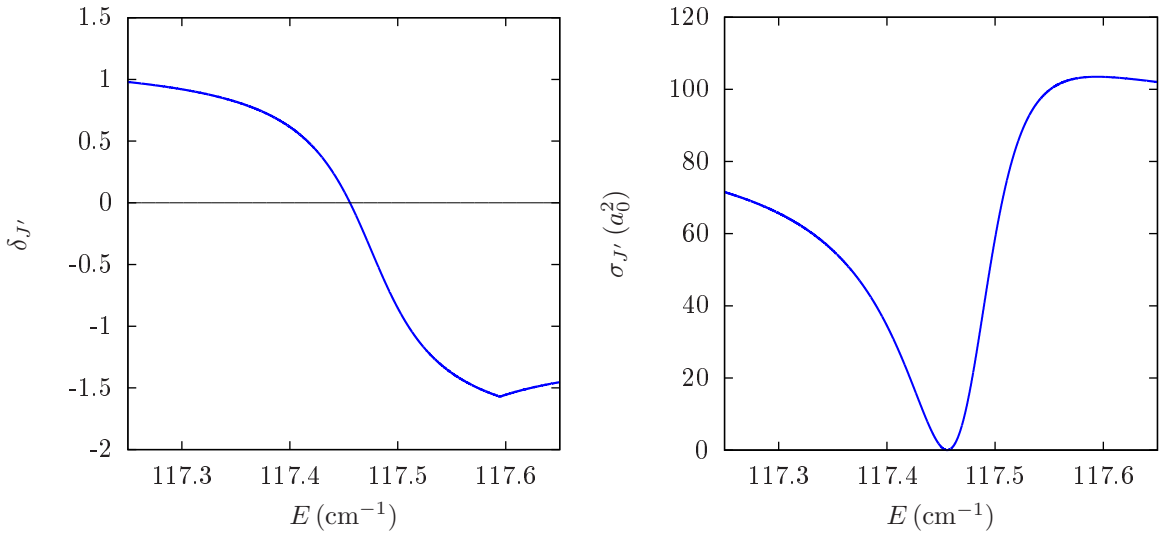

Figure 3.4: Computed phase shift and partial ($J' = 20$) scattering cross section resonance line shape on vibrational manifold $v' = 0$.

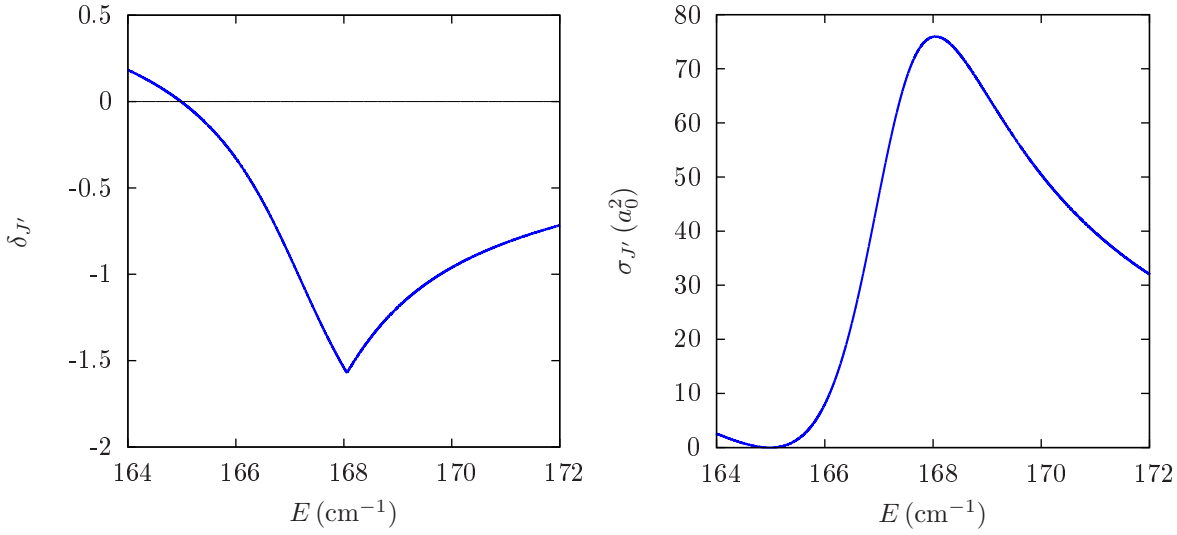

Figure 3.5: Computed phase shift and partial ($J' = 21$) scattering cross section resonance line shape on vibrational manifold $v' = 0$.

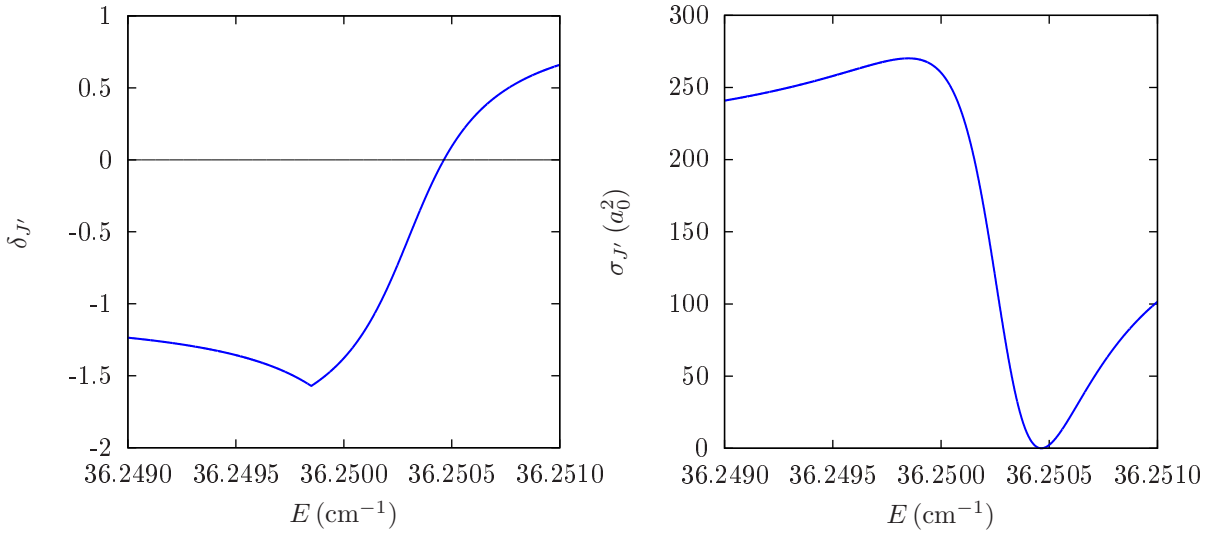

Figure 3.6: Computed phase shift and partial ($J' = 16$) scattering cross section resonance line shape on vibrational manifold $v' = 1$.

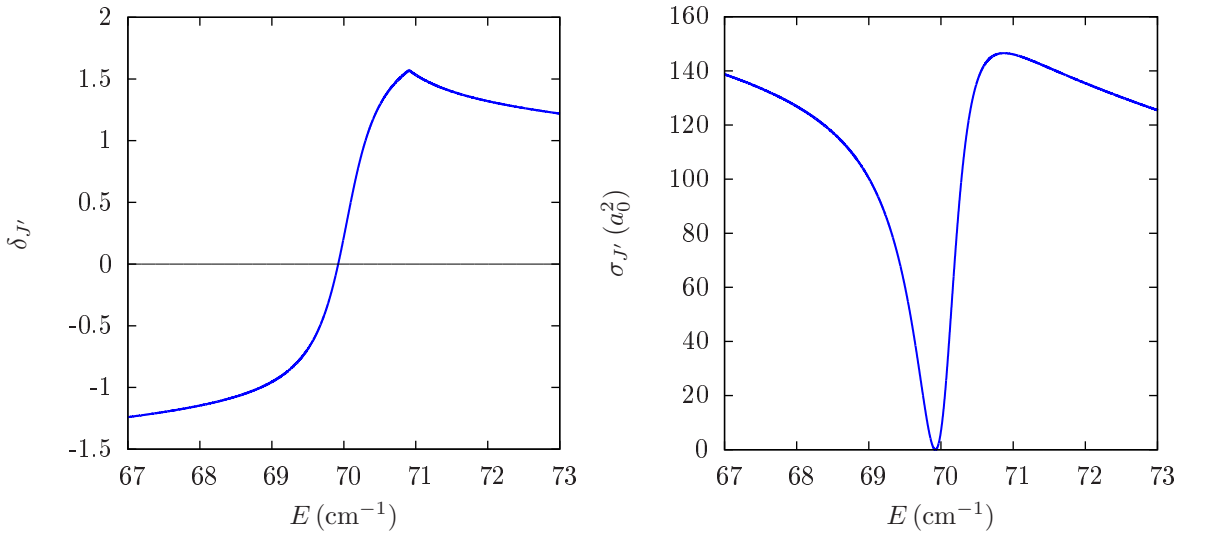

Figure 3.7: Computed phase shift and partial ($J' = 17$) scattering cross section resonance line shape on vibrational manifold $v' = 1$.

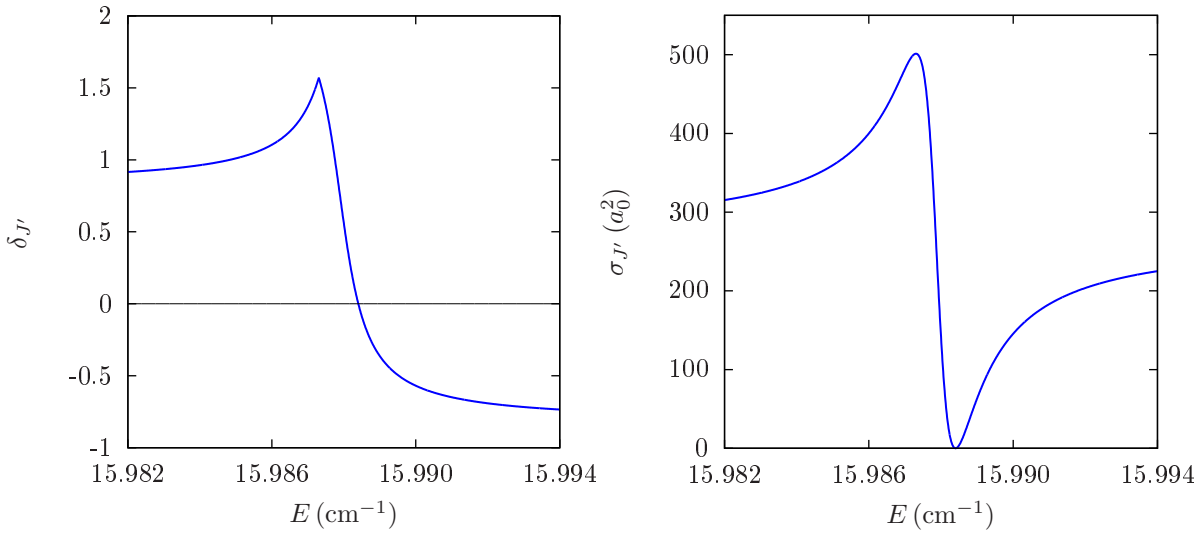

Figure 3.8: Computed phase shift and partial ($J' = 13$) scattering cross section resonance line shape on vibrational manifold $v' = 2$.

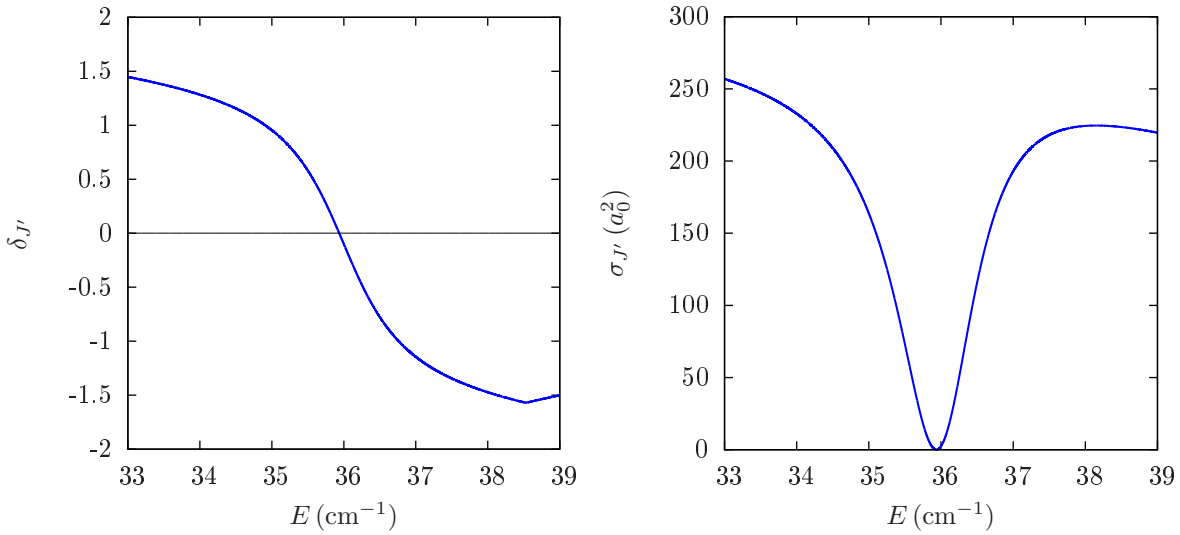

Figure 3.9: Computed phase shift and partial ($J' = 14$) scattering cross section resonance line shape on vibrational manifold $v' = 2$.

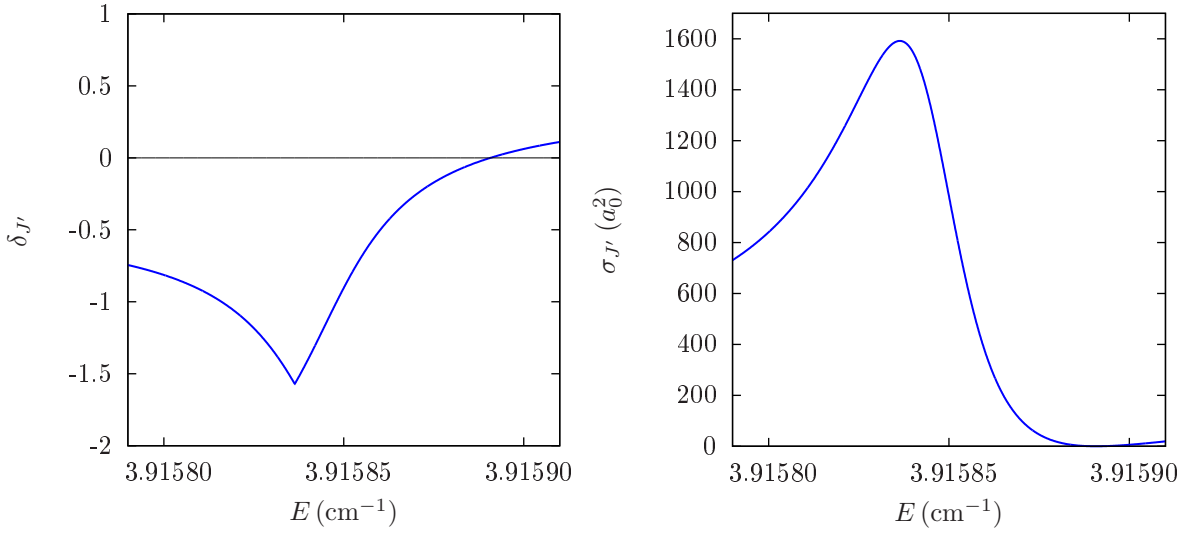

Figure 3.10: Computed phase shift and partial ($J' = 10$) scattering cross section resonance line shape on vibrational manifold $v' = 3$.

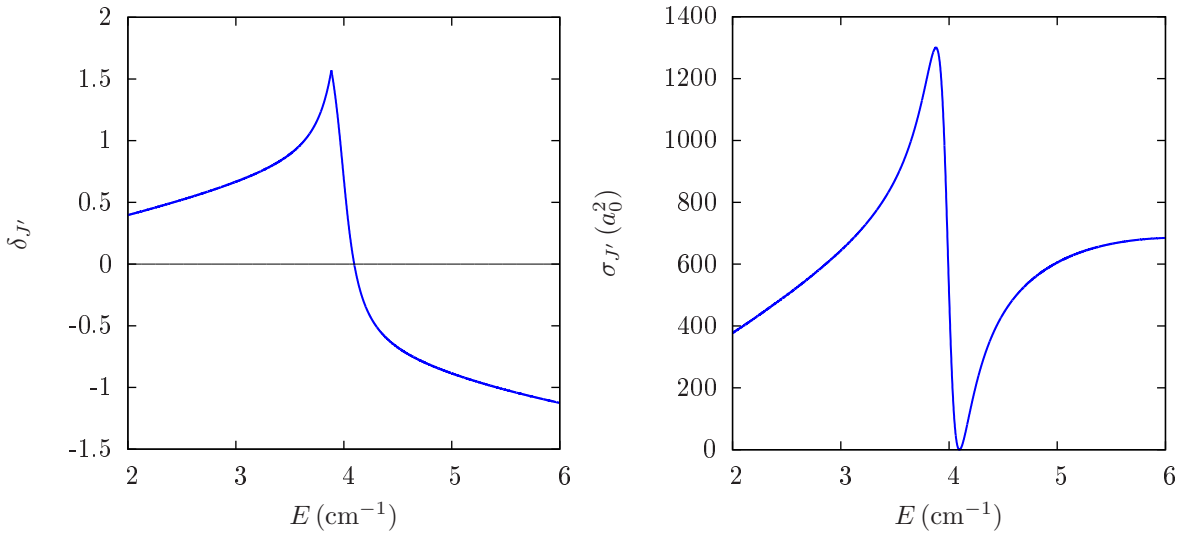

Figure 3.11: Computed phase shift and partial ($J' = 8$) scattering cross section resonance line shape on vibrational manifold $v' = 4$.

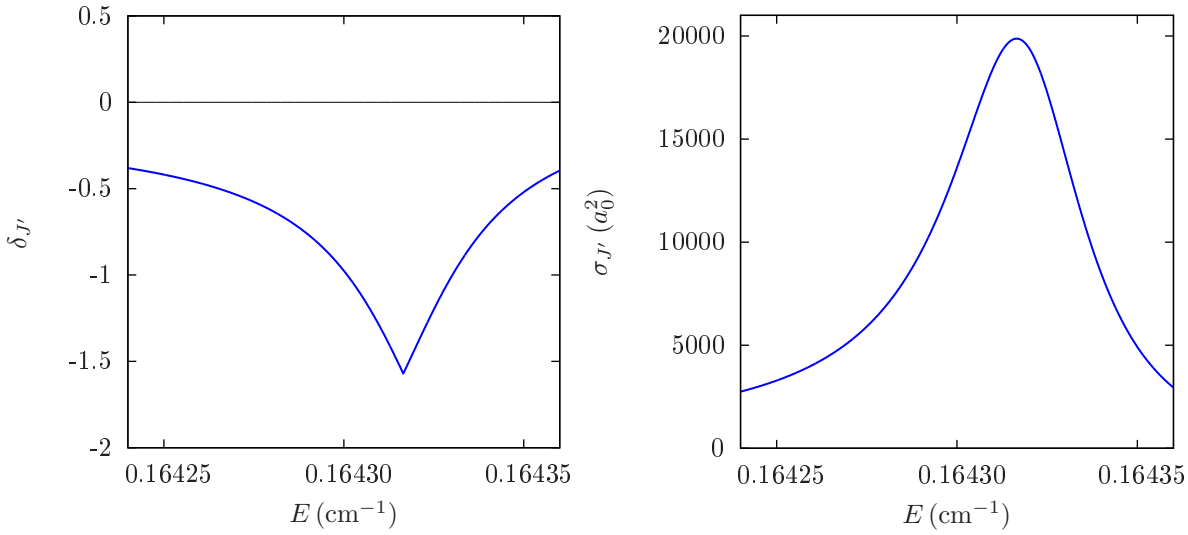

Figure 3.12: Computed phase shift and partial ($J' = 5$) scattering cross section resonance line shape on vibrational manifold $v' = 5$.

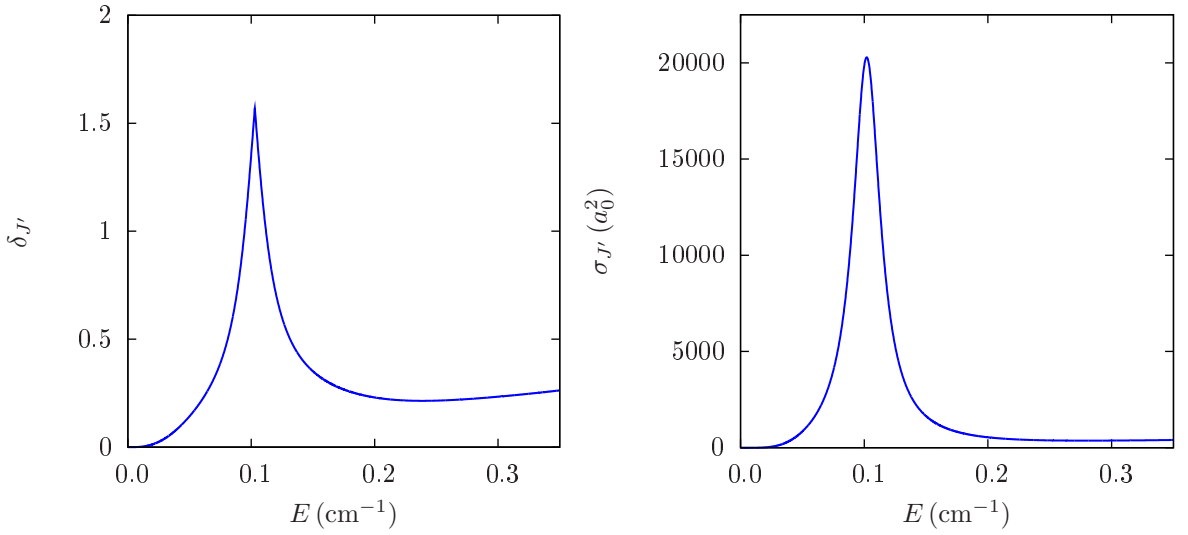

Figure 3.13: Computed phase shift and partial ($J' = 3$) scattering cross section resonance line shape on vibrational manifold $v' = 6$.

As we can see, there is a good agreement between the semiclassical results of LEVEL 7.7 and the results of our scattering calculations.

3.2.2 The cross sections for radiative association

In Fig. 3.14 we illustrate the evaluated radiative cross section for process (3.1) for different collision energy values in the interval between $10^{-2}\,\mathrm{cm}^{-1}$ and $10^{4}\,\mathrm{cm}^{-1}$. The partial cross sections as a function of energy, $\sigma_{v''}(E)$, for radiative association to form LiHe^{+} ($X\,^{1}\Sigma^{+}$) are shown in Figures 3.15 – 3.21. From the listed results, we observe that the partial cross sections exhibit a very strong dependence on the final vibrational state into which the molecular ion is formed after the photon emission.

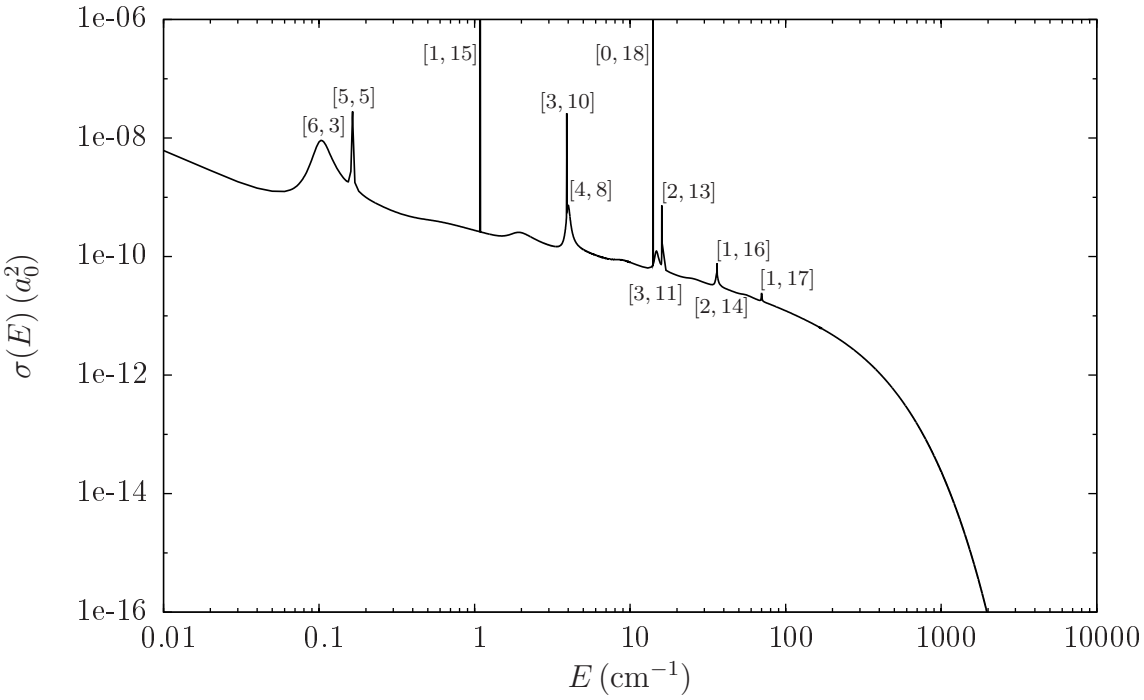

Figure 3.14: The total cross section for radiative association of $\mathrm{Li}^{+}(1s^2)+\mathrm{He}(1s^2)$ in a.u. as a function of relative energy. The peaks represent contribution of resonant states $[v', J']$.

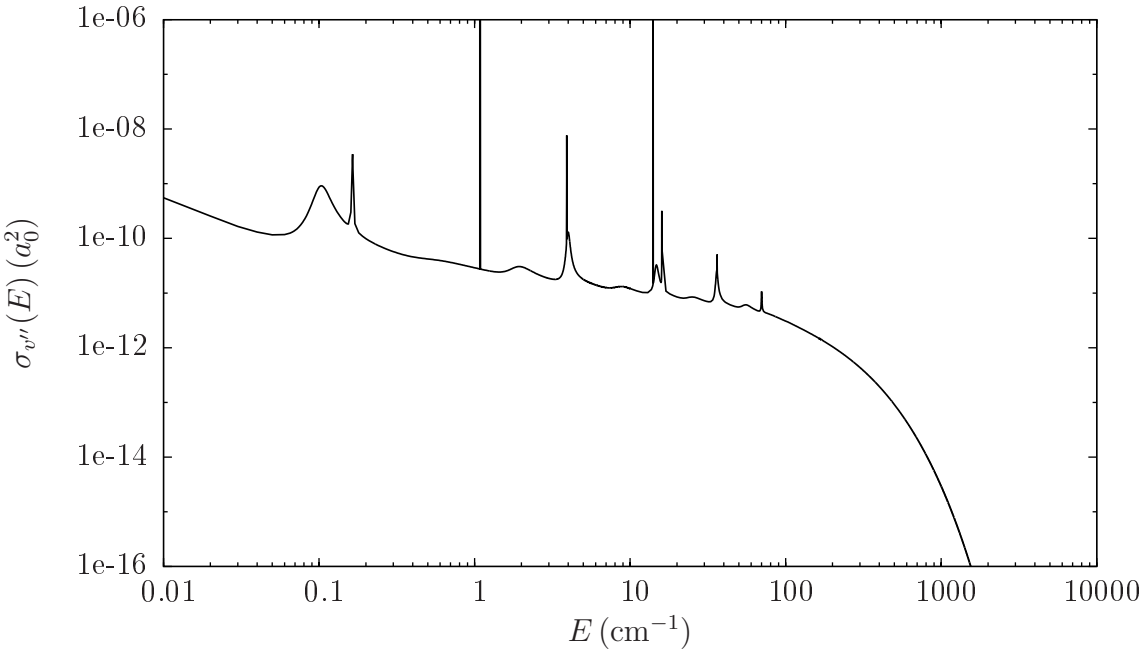

Figure 3.15: Computed partial cross section for radiative association of $\mathrm{Li}^+(1s^2) + \mathrm{He}(1s^2)$ in a.u. as a function of relative energy for the final vibrational state $v'' = 0$.

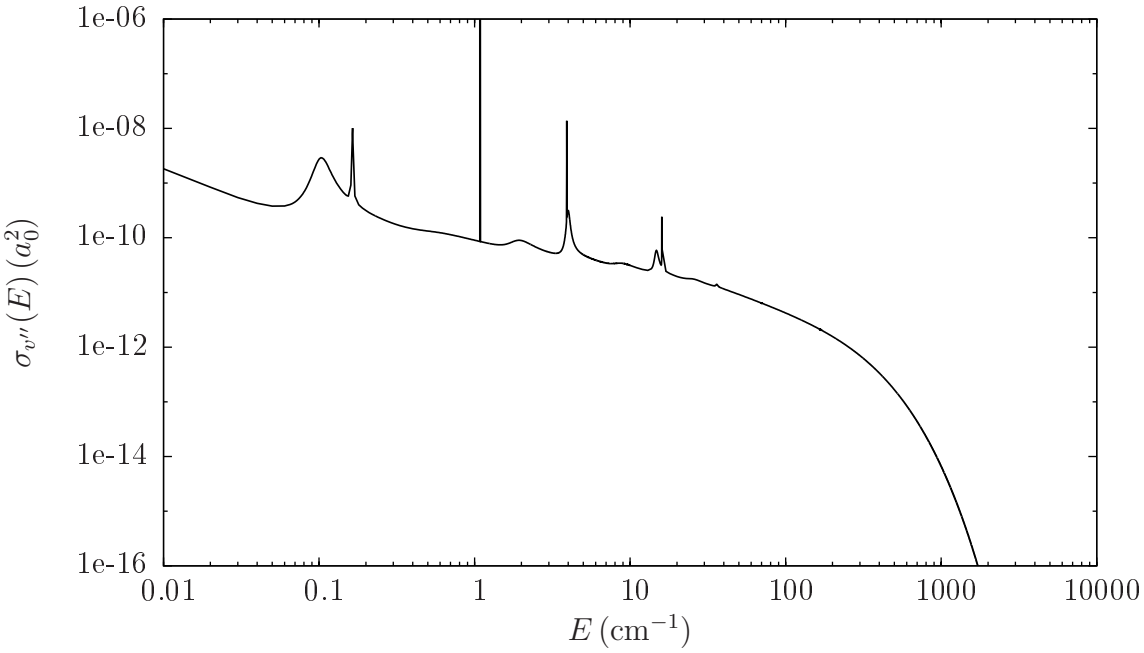

Figure 3.16: Computed partial cross section for radiative association of $\mathrm{Li}^+(1s^2) + \mathrm{He}(1s^2)$ in a.u. as a function of relative energy for the final vibrational state $v'' = 1$.

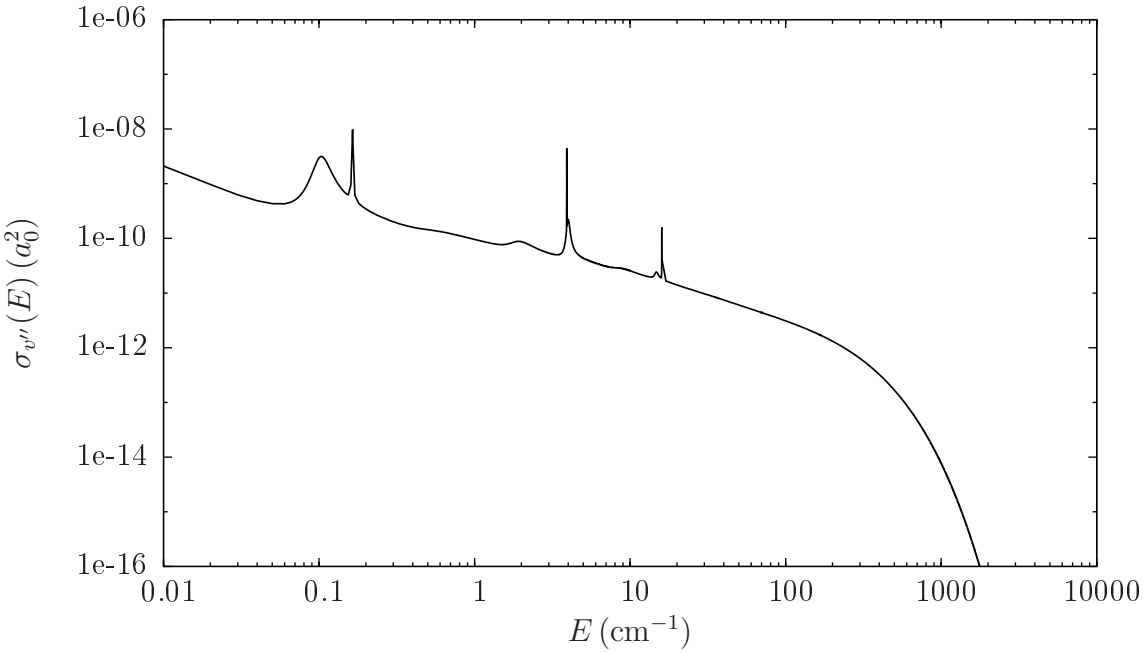

Figure 3.17: Computed partial cross section for radiative association of $\mathrm{Li}^+(1s^2) + \mathrm{He}(1s^2)$ in a.u. as a function of relative energy for the final vibrational state $v'' = 2$.

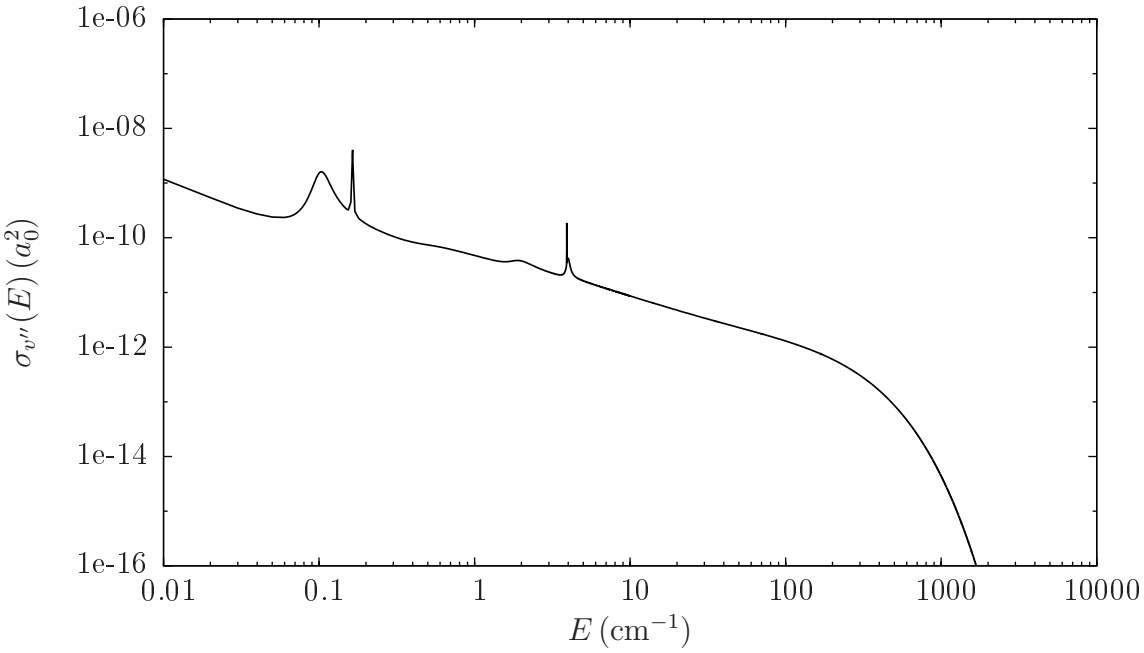

Figure 3.18: Computed partial cross section for radiative association of $\mathrm{Li}^+(1s^2) + \mathrm{He}(1s^2)$ in a.u. as a function of relative energy for the final vibrational state $v'' = 3$.

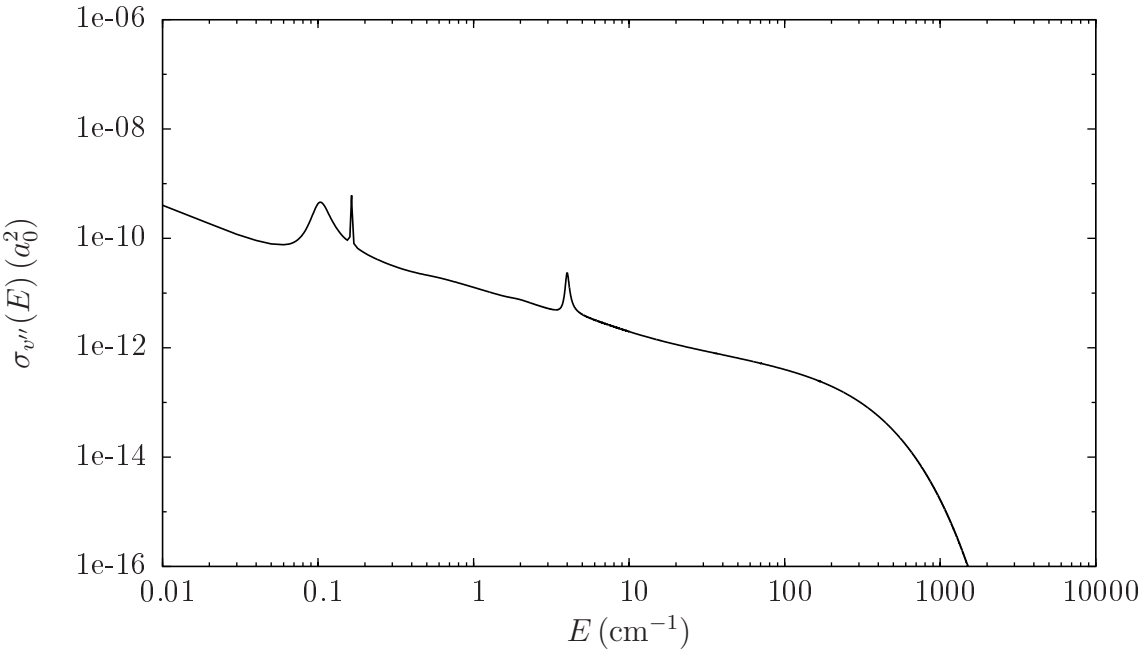

Figure 3.19: Computed partial cross section for radiative association of $\mathrm{Li}^+(1s^2) + \mathrm{He}(1s^2)$ in a.u. as a function of relative energy for the final vibrational state $v'' = 4$.

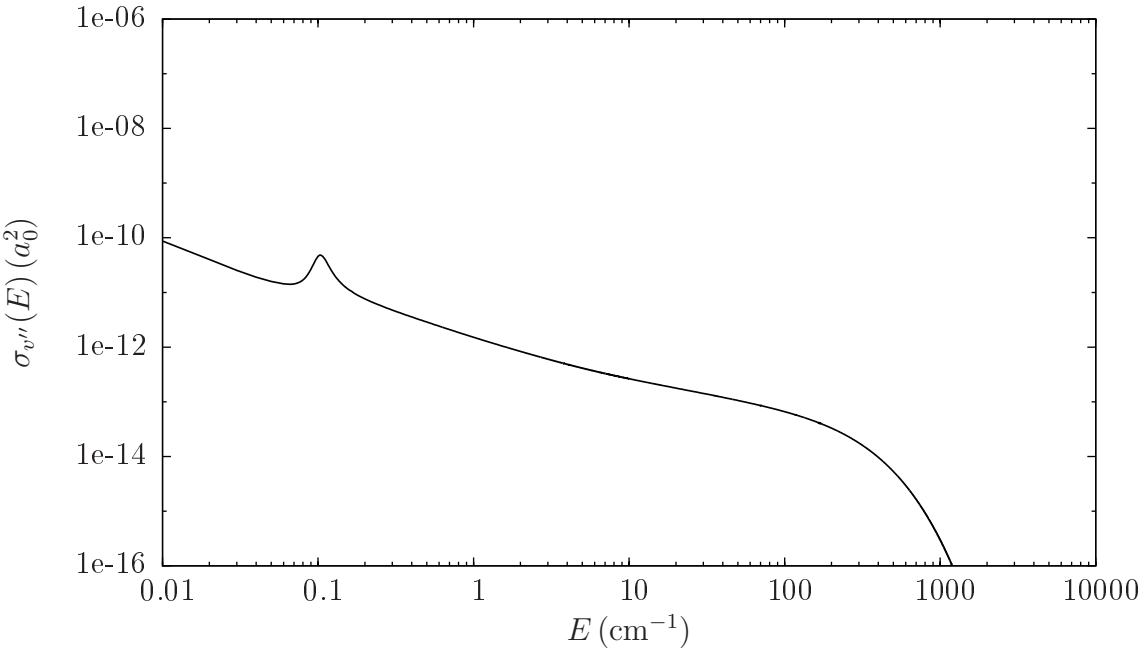

Figure 3.20: Computed partial cross section for radiative association of $\mathrm{Li}^+(1s^2) + \mathrm{He}(1s^2)$ in a.u. as a function of relative energy for the final vibrational state $v'' = 5$.

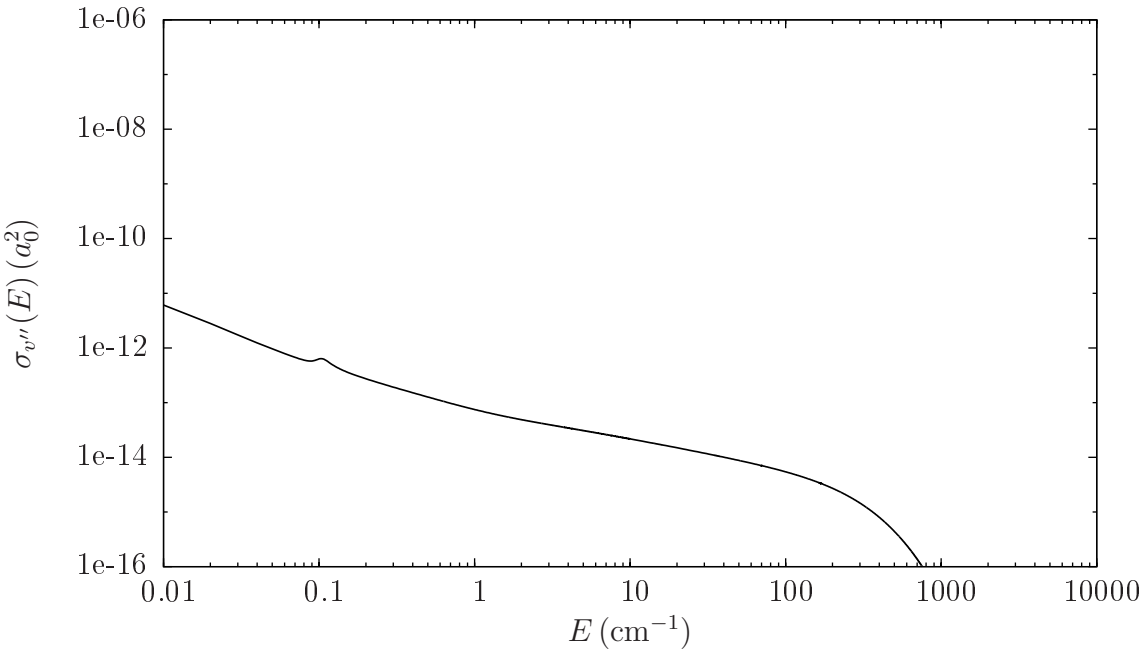

Figure 3.21: Computed partial cross section for radiative association of $Li^+(1s^2)$ + $He(1s^2)$ in a.u. as a function of relative energy for the final vibrational state $v'' = 6$.

Chapter 4

Conclusion and further perspectives

In this diploma thesis we dealt with the phenomenon of radiative association in the case of diatomic molecules. The role of potential barrier in a resonance scattering was briefly discussed on a model example. Hönl-London coefficients for dipole moment and quadrupole moment transitions were derived. We carried out quantum-mechanical calculations for direct radiative association of the $\mathrm{LiHe}^+(X\,^1\Sigma^+)$ molecular ion starting from $\mathrm{Li}^+(1s^2)+\mathrm{He}(1s^2)$. The dipole moment transition considered is from the ground electronic state to the ground electronic state, *i.e.*, $X \to X$ process. In near future our study will be extended to the processes

$$\begin{aligned}
\mathrm{Li}(1s^2\,2s) + \mathrm{He}^+(1s) &\to \mathrm{LiHe}^+(X\,^1\Sigma^+) + h\nu, \quad A \to X\,,\\
\mathrm{Li}(1s^2\,2s) + \mathrm{He}^+(1s) &\to \mathrm{LiHe}^+(A\,^1\Sigma^+) + h\nu, \quad A \to A\,,\\
\mathrm{Li}(1s^2\,2s) + \mathrm{He}^+(1s) &\to \mathrm{LiHe}^+(a\,^3\Sigma^+) + h\nu, \quad a \to a\,.
\end{aligned}$$

In future we would like to investigate the process of radiative association of He_2^+, particularly

$$\begin{aligned}
\mathrm{He}(1s^2) + \mathrm{He}^+(1s) &\to \mathrm{He}_2^+(X\,^2\Sigma_u^+) + h\nu, \quad X \to X\,,\\
\mathrm{He}(1s^2) + \mathrm{He}^+(1s) &\to \mathrm{He}_2^+(X\,^2\Sigma_u^+) + h\nu, \quad A \to X\,,\\
\mathrm{He}(1s^2) + \mathrm{He}^+(1s) &\to \mathrm{He}_2^+(A\,^2\Sigma_g^+) + h\nu, \quad A \to A\,.
\end{aligned}$$

Bibliography

[1] L. Augustovičová, *Non-analytical methods for the time-independent one-dimensional Schrödinger equation*, Bakalářská práce, ČVUT, Fakulta jaderná a fyz. inženýrská, Katedra fyziky, Praha, 2009.

[2] L. Augustovičová and P. Soldán, *unpublished results.*

[3] O. J. Bennett, A. S. Dickinson, T. Leininger, and F. X. Gadéa, *Radiative association in Li+H revisited: the role of quasi-bound states*, Mon. Not. R. Astron. Soc., 341 (2003), pp. 361–368.

[4] J. Brown and A. Carrington, *Rotational Spectroscopy of Diatomic Molecules*, Cambridge University Press, 2003.

[5] M. S. Child, *Molecular Collision Theory*, Dover, 1996.

[6] E. U. Condon and G. H. Shortley, *The Theory of Atomic Spectra*, Cambridge University Press, Cambridge, 1935.

[7] J. Cooley, *An improved eigenvalue corrector formula for solving the schrödinger equation for central fields*, Math. Comput., 15 (1961), pp. 363–374.

[8] A. Dalgarno, *Molecular processes in the early Universe*, J. Phys.: Conf. Ser., 4 (2005), pp. 10–16.

[9] A. Dalgarno, K. Kirby, and P. C. Stancil, *The radiative association of Li^+ and H, Li and H^+, and Li and H*, Astrophys. J., 458 (1996), pp. 397–400.

[10] A. R. Edmonds, *Angular Momentum in Quantum Mechanics*, Princeton Univ. Press, Princeton, New Jersey, 1960.

[11] D. R. Farley and R. J. Cattolica, *Multipole line strengths for linear Hund's case (a) molecules*, J. Quant. Spectrosc. Radiat. Transfer, 56 (1996), pp. 753–760.

[12] J. Formánek, *Úvod do kvantové teorie*, Academia, Praha, 1983.

[13] D. Gerlich and S. Horning, *Experimental investigation of radiative association processes as related to interstellar chemistry*, Chem. Rev, 92 (1992), pp. 1509–1539.

[14] F. A. Gianturco and P. G. Giorgi, *Radiative association of LiH ($X\ ^1\Sigma^+$) from electronically excited lithium atoms*, Phys. Rev. A, 54 (1996), pp. 4073–4077.

[15] F. A. Gianturco and P. G. Giorgi, *Radiative association rates and structure of resonances for Li and Li^+ colliding with H and H^+*, Astrophys. J., 479 (1997), pp. 560–567.

[16] I. I. Gol'dman and V. D. Krivchenkov, *Problems in Quantum Mechanics*, Pergamon Press, 1961.

[17] R. J. Le Roy, *A computer program for solving the radial Schrödinger equation for bound and quasibound levels*, Technical Report CP-642R^3, University of Waterloo, 2001.

[18] R. J. Le Roy and W.-K. Liu, *Energies and widths of quasibound levels (orbiting resonances) for spherical potentials*, J. Chem. Phys., 69 (1978), pp. 3622–3631.

[19] S. Lepp, P. C. Stancil, and A. Dalgarno, *Atomic and molecular processes in the early Universe*, J. Phys. B: At. Mol. Opt. Phys., 35 (2002), pp. 57–80.

[20] T. E. Simos, *Eighth order methods for accurate computations for the Schrödinger equation*, Comput. Phys. Commun., 105 (1997), pp. 127–138.

[21] P. Soldán, *unpublished results.*

[22] P. C. Stancil, J. F. Babb, and A. Dalgarno, *The radiative association of He^+ and He and H^+ and H*, Astrophys. J., 414 (1993), pp. 672–675.

[23] P. C. Stancil, S. Lepp, and A. Dalgarno, *The lithium chemistry of the early Universe*, Astrophys. J., 458 (1996), pp. 401–406.

[24] J. K. G. Watson, *The isotope dependence of diatomic Dunham coefficients*, J. Mol. Spectrosc., 80 (1980), pp. 411–421.

[25] B. Zygelman and A. Dalgarno, *The radiative association of He^+ and H*, Astrophys. J., 365 (1990), pp. 239–240.

Prohlášení

Prohlašuji, že jsem svou diplomovou práci vypracovala samostatně a použila jsem pouze podklady uvedené v přiloženém seznamu.

Nemám žádný důvod proti užití tohoto školního díla ve smyslu §60 Zákona č. 121/2000 Sb., o právu autorském, o právech souvisejících s právem autorským a o změně některých zákonů (autorský zákon).

Declaration

I declare that I wrote my diploma thesis independently and exclusively with the use of cited bibliography.

I agree with the usage of this thesis in a purport of the Act 121/2000 (Copyright Act).

Praha, May 5, 2011

Lucie Augustovičová